HHS Public Access

Author manuscript

Eur J Immunol. Author manuscript; available in PMC 2025 December 01.

Published in final edited form as:

Eur J Immunol. 2024 December ; 54(12): e2451245. doi:10.1002/eji.202451245.

A20 intrinsically influences human effector T cell survival and function by regulating both NF-κB and JNK signaling

Gina Dabbah-Krancher[1,2], **Allison Ruchinskas**[1,2], **Melissa A. Kallarakal**[1], **Katherine P. Lee**[1], **Bradly M. Bauman**[1,2], **Benjamin Epstein**[1,2], **Hongli Yin**[3], **Daniel Krappmann**[3], **Brian C. Schaefer**[4], **Andrew L. Snow**[1,*]

[1]Department of Pharmacology & Molecular Therapeutics, Uniformed Services University of the Health Sciences; Bethesda, MD, USA

[2]Henry M. Jackson Foundation for the Advancement of Military Medicine; Bethesda, MD, USA

[3]Research Unit Signaling and Translation, Molecular Targets and Therapeutics Center, Helmholtz Zentrum München, German Research Center for Environmental Health; Neuherberg 85764, Germany

[4]Department of Microbiology and Immunology, Uniformed Services University of the Health Sciences; Bethesda, MD, USA

Abstract

A20 is a dual-function ubiquitin-editing enzyme that maintains immune homeostasis by restraining inflammation. Although A20 serves a similar negative feedback function for T cell receptor (TCR) signaling, the molecular mechanisms utilized and their ultimate impact on human T cell function remain unclear. TCR engagement triggers the assembly of the CARD11-BCL10-MALT1 (CBM) protein complex, a signaling platform that governs the activation of downstream transcription factors including NF-κB and c-Jun/AP-1. Utilizing WT and A20 knockout Jurkat T cells, we found that A20 is required to negatively regulate both NF-κB *and* JNK. Utilizing a novel set of A20 mutants in NF-κB and AP-1 driven reporter systems, we discovered the ZnF7 domain is crucial for negative regulatory capacity, while deubiquitinase activity is dispensable. Successful inactivation of A20 in human primary effector T cells congruently conferred sustained NF-κB and JNK signaling, including enhanced upregulation of activation markers, and increased secretion of several cytokines including IL-9. Finally, loss of A20 in primary human T cells resulted in decreased sensitivity to restimulation induced cell death (RICD) and increased sensitivity to cytokine withdrawal induced death (CWID). These findings demonstrate the importance of A20 in maintaining T cell homeostasis via negative regulation of both NF-κB and JNK signaling.

Graphical Abstract

*Corresponding author. andrew.snow@usuhs.edu.

AUTHOR CONTRIBUTIONS

Gina Dabbah-Krancker designed and performed the experiments, prepared figures and wrote the manuscript. Allison Ruchinskas, Melissa Kallarakal, Katherine Lee, Bradly Bauman and Benjamin Epstein contributed to some experiments. Hongli Yin and Daniel Krappmann provided Jurkat T cell lines, consulted on key experiments and helped edit the manuscript. Brian Schaefer helped supervise the research and edited the manuscript. Andrew Snow supervised and funded the research and edited the manuscript.

CONFLICT OF INTEREST

The authors declare no commercial or financial conflict of interest.

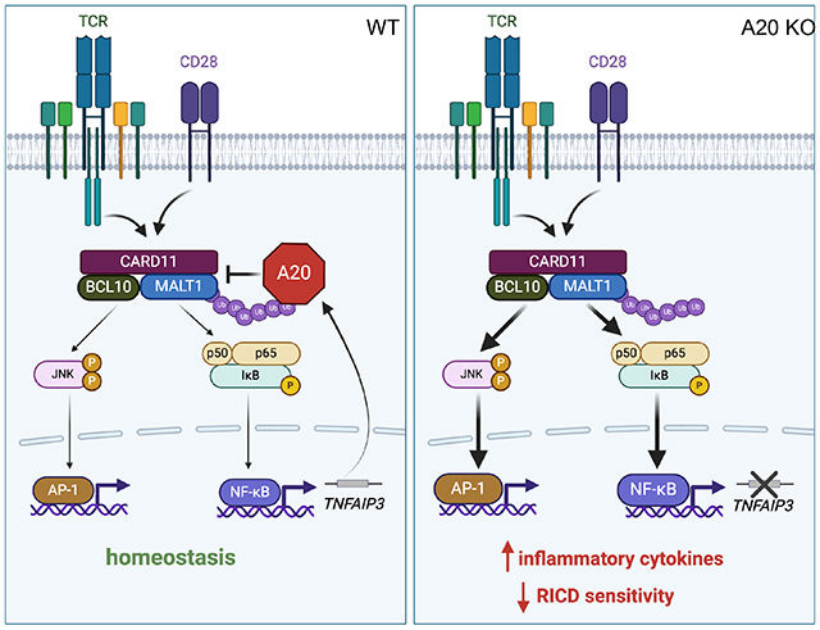

The ubiquitin-editing enzyme A20 regulates innate and adaptive immune receptor signaling, but its intrinsic function in human T cells is poorly understood. Here we show that A20 deletion enhances cytokine secretion and alters apoptosis sensitivity in primary human T cells by modulating both NF-kB and JNK/AP-1 signaling downstream of the CARD11-BCL10-MALT1 complex.

INTRODUCTION

The tumor necrosis factor alpha-induced protein 3 (*TNFAIP3*) gene encodes the protein A20, a ubiquitous dual-function ubiquitin-editing enzyme that modulates NF-κB signaling, restrains inflammation, and maintains immune homeostasis [1–3]. In many cell types, A20 is upregulated in an NF-κB-dependent manner to negatively modulate signaling through innate immune sensors and cytokine receptors including toll-like receptors (TLRs), NOD-like receptors (NLRs), tumor necrosis factor receptor 1 (TNFR1), and interleukin-1 receptor (IL-1R) [2, 4–11]. The A20 open reading frame (ORF) includes an N-terminal ovarian tumor (OTU) domain with intrinsic deubiquitinase (DUB) activity, coupled to seven zinc finger (ZnF) domains that contain E3 ligase activity and/or ubiquitin binding capacity. Depending on the specific upstream signal, A20 may rely on the coordinated function of these domains to regulate ubiquitinylated signalosomes to dampen downstream NF-κB signaling [2, 3, 12, 13].

Enhanced, uncontrolled TNF-induced NF-κB signaling is observed in A20-deficient mice, which die prematurely from hyperinflammation, cachexia, and severe tissue damage affecting multiple organs [7]. In humans, heterozygous loss-of-function (LOF) mutations in A20 result in A20 haploinsufficiency (HA20), a systemic autoinflammatory disease presenting early in life with recurrent fevers, oral/genital/gastrointestinal ulcers, skin lesions and dermal abscesses, and musculoskeletal disorders, often initially diagnosed as an atypical

form of Behçet's disease (BD) [14–18]. Subsets of HA20 patients also exhibit signs of lymphoproliferation (e.g. lymphadenopathy) and autoimmunity (27% harbor autoantibodies) [19]; indeed, single nucleotide polymorphisms (SNPs) around the *TNFAIP3* locus have been associated with autoimmune diseases in the general population such as rheumatoid arthritis, and/or systemic lupus erythematosus (SLE) [20–23]. Patient PBMCs show little to no expression of A20, leading to increased NF-κB activation at baseline with sustained signaling post-TNF stimulation [14]. Indeed, systemic inflammation in HA20 is thought to be driven primarily by innate immune dysregulation, given that loss of lymphocytes via RAG1 deficiency does not appreciably ameliorate disease in A20 knockout mice [7]. However, mice lacking A20 expression in B cells exhibited spontaneous B cell activation, expansion of germinal center B cells, and production of autoantibodies [10, 11, 24]. Similarly, loss of A20 in aged murine B cells was shown to lower their activation threshold, increase NF-κB signaling, and enhance proliferation and survival, including resistance to Fas-mediated apoptosis [10, 11]. These data collectively suggest that A20 acts to restrict B cell growth, survival, and transformation by modulating NF-κB activity and facilitating cell death (including for autoreactive B cells). Nevertheless, it remains unclear whether abnormal adaptive immunity may also contribute to clinical disease in HA20, demanding further investigation.

A20 is constitutively expressed in lymphocytes and further upregulated shortly after antigen receptor ligation, helping to terminate NF-κB signaling for proper control of B and T cell activation [1]. A20 was identified as a tumor suppressor gene that is frequently (~30%) inactivated gene in human B cell lymphomas thought to exhibit oncogenic addiction to constitutive NF-κB stimulation [25, 26]. Ectopic reintroduction of A20 into B- and T-cell cancer lines lacking endogenous expression decreased cell proliferation and increased apoptotic cell death. Similar to human CD4+ T cells [27], conditional A20 deletion in murine CD8+ T cells results in enhanced NF-κB signaling and elevated production of IL-2, IFN-γ, and TNF-α [28, 29]. HA20 patient CD4+ T cells show evidence of increased polarization toward Th9 and Th17 effector cell lineages ex vivo, hypothesized to be linked in part to elevated IL-1β signaling [14]. Although these previous findings offer tantalizing clues, the intrinsic effects of A20 deletion on the survival, proliferation and function of primary human T cells remains poorly understood.

Immediately following T-cell receptor (TCR) stimulation, the CARD11-BCL10 (B cell lymphoma 10)-MALT1 (mucosa-associated lymphoid tissue lymphoma translocation protein 1) (CBM) complex assembles to trigger several downstream signaling pathways including NF-κB, c-Jun N-terminal kinase (JNK), and mTORC1 [30–34]. The active CBM complex becomes highly ubiquitinated and acts as a recruiting platform for IκB kinase (IKK), culminating in the phosphorylation and degradation of IκBα, and release of NF-κB dimers into the nucleus [35, 36]. Pre-existing A20 protein is rapidly lost via proteosome-directed degradation, but is quickly resynthesized when NF-κB binds to -κB elements in *TNFAIP3* promoter to induce expression [31]. Several prior studies indicate A20 is an important negative feedback regulator of the CBM complex, but the actual mechanism remains nebulous. Early biochemical investigations were often performed in non-lymphoid cells such as 293T, which do not always accurately predict results in T cells. One study demonstrated A20 could remove K63-linked ubiquitin chains attached to MALT1 in a cell-free assay,

which was assumed to preclude further recruitment and activation of signaling partners to the CBM complex [35]. However, the DUB activity of A20 was recently confirmed to be dispensable for TCR signal regulation [2, 3, 27, 37, 38]. Moreover, MALT1 protease can cleave A20 at arginine 439, which helps to sustain TCR signal propagation [35]. In non-lymphoid cells, ZnF4 was shown to bind mono-ubiquitin and possess E3 ligase activity, allowing the addition of K48-linked ubiquitin to terminate NF-κB signaling [12, 27]. Congruently, ZnF7 has been shown to bind M1-linked (linear) ubiquitin chains [39, 40]. A recent report demonstrated that mutation of ZnF4/7 sites precluded A20 recruitment to the CBM complex [27], although the precise role of each ZnF domain for TCR-induced NF-κB regulation has yet to be dissected. Moreover, the role of A20 in modulating other CBM-dependent signal outputs like JNK/c-Jun has not been investigated.

In this study, we sought to address the central unresolved question of how A20-mediated regulation of CBM-dependent signaling pathways ultimately affects intrinsic human T cell activation *and* function. Utilizing Jurkat T cells, we discovered a role for A20 in modulating TCR-induced activation of both transcription factors NF-κB and c-Jun/AP-1 downstream of the CBM complex, largely through a non-enzymatic function requiring the zinc finger 7 (ZnF7) domain. We also employed a novel CRISPR/Cas9-based strategy to delete A20 in primary human T cells to assess intrinsic impacts on effector T cell survival and function. Inactivation of A20 enhanced TCR-mediated NF-κB and JNK signaling and produced marked changes in cytokine secretion and apoptosis sensitivity, highlighting an intrinsic role for A20 in regulating human T cell fate.

MATERIALS AND METHODS

Immunoblot analysis and quantification

For immunoblot analysis, cell lysates were prepared with NP-40 lysis buffer (50 mM Tris pH 7.4, 0.5 mM EDTA, 150 mM NaCl, 1% NP-40, and 0.5% deoxycholate) with protease and phosphatase inhibitor cocktails added (Sigma). Lysates were separated on 10% or 4-20% Tris-glycine gels (Bio-Rad or Invitrogen) and transferred to nitrocellulose using a Trans-Blot Turbo transfer system (Bio-Rad). Incubation with primary antibodies (Abs) was followed by incubation with anti-mouse or anti-rabbit secondary Abs conjugated to IRDye680 or IRDye800 (LI-COR; 1:10,000) prior to imaging on an Odyssey CLx infrared imaging system (LI-COR Biosciences). Primary Abs used for immunoblots included anti-FLAG/DYKDDDDK Tag (9A3), anti-Myc-tag (71D10), anti-IκBα, anti-A20/TNFAIP3 (D13H3), anti-phospho-c-Jun (Ser63), anti-phospho-SAPK/JNK (Thr183/Tyr185), anti-c-Jun (L70B11) from Cell SignalingTechnologies, A20/TNFAIP3 (59A426; ThermoFisher) and β-actin (AC-15; Sigma). All Ab clones used in this study are listed in Table 1. Protein bands were quantified using spot densitometry on the Odyssey system (LiCOR); target protein bands were normalized to β-actin bands as a loading control.

Cloning and mutagenesis

All primer sequences used for cloning and site-directed mutagenesis are listed in Table 2. Constructs for the expression of A20 were derived from pEGFP-C1-A20, a gift from Yihong Ye (Addgene plasmid # 22141) [41]. First, the coding sequence for A20 was

amplified from pEGFP-C1-A20 using A20 Amp Forward and Reverse primers. The 3x FLAG tag was amplified from pUNO-CARD11-3x FLAG using 3x FLAG Amp Forward and Reverse primers, adding complementary bases to both the 5' and 3' ends for construct assembly [42]. The 3x MYC tag was amplified from previously described plasmid using 3x MYC Amp Forward and Reverse primers, again adding complementarity for construct assembly [43]. The dual-tagged 3x MYC-A20-3x FLAG construct was assembled using the NEBuilder HiFi DNA Assembly Master Mix according to the manufacturer's instructions (New England BioLabs, NEB) by combining the amplified 3x MYC, A20, and 3x FLAG fragments with the pUNO1-Empty Vector construct (InvivoGen) after digestion with SgrAI and NheI. Successful assembly was confirmed via Sanger sequencing.

Subsequently, site-directed mutagenesis was performed using Phusion DNA polymerase (Invitrogen) for linear amplification followed by DpnI digest as previously described, for the generation of a suite of novel A20 expression constructs [42]. A non-cleavable A20 construct, in which the MALT1-dependent cleavage site is mutated (non-cleavable; R439A), was generated with Non-cleavable Forward and Reverse primers. E3 ligase activity was removed by mutating ZnF4 (mZnF4; C609A/C612A) with mZnF4 Forward and Reverse primers, and M1-linear ubiquitin binding activity was removed by mutating ZnF7 (mZnF7; C764A/C767A) with mZnF7 Forward and Reverse primers. Similarly, the OTU domain was mutated to abolish deubiquitinase (mDUB) activity with mDUB Forward and Reverse primers. Site-directed mutagenesis was also used to insert a stop codon at the end of A20 or remove the start codon of the 3x MYC tag, generating constructs for singly tagged A20 (3x MYC-A20 or A20-3x FLAG, respectively). Use of both sets of primers generated a tagless A20 construct. To assay functional differences between the mutation of active sites in key domains and the loss of those domains entirely, several key domains were removed via PCR amplification and ligation using 5'-phosphorylated forward primers (A20 delta OTU, ZnF4, ZnF7). Similarly, constructs expressing only the N- and C-terminal A20 fragments after MALT1 cleavage were also generated via PCR and ligation with 5'-phosphorylated primers (A20 N- and C-term fragments).

Mutations were confirmed by Sanger sequencing (Psomagen), and all plasmids were isolated for transfection from transformed competent NEB 5-alpha *E. coli* (New England BioLabs) using a GenElute HP Plasmid MaxiPrep kit (Sigma). To construct our novel NF-κB-GFP reporter, we began with the pGL4.32 NF-κB-driven luciferase reporter (Promega) as a template, and all PCR amplification steps were performed using Phusion DNA polymerase. First, we removed the luciferase expression cassette and replaced it with green fluorescent protein 2 (GFP2; also called ppluGFP2 and copGFP; from *Pontellina plumata*) [44], which was cloned out of the pmaxGFP vector (Lonza) using GFP2 Forward and Reverse primers (Table 1). The pGL4.32 backbone was linearized, including the PEST destabilization domain, with NF-κB Backbone Forward and Reverse primers. The amplified segments were assembled using the NEBuilder HiFi DNA Assembly Master Mix (NEB), and successful insertion of GFP2 was confirmed by Sanger sequencing. This NF-κB-GFP reporter was used as template for generation of the AP-1 reporter. The NF-κB Response Element (RE) was removed via linear amplification with RE Excision Forward and Reverse primers. The AP-1 RE was constructed with a 6x repeat of the AP-1 consensus site, TGAC/GTCA [45], via annealing and amplification of the AP-1 RE Forward and Reverse primers. Assembly of

the backbone and RE fragments was performed with the NEBuilder HiFi DNA Assembly Master Mix, and successful insertion of the RE was confirmed by Sanger sequencing.

Cell line culture and transfection

WT and A20 KO Jurkat T cell lines were generously provided by Dr. Daniel Krappmann [27]. All Jurkat cells were cultured in complete RPMI 1640 medium (Gibco) supplemented with 1% penicillin-streptomycin (Gibco), 10% fetal bovine serum (FBS; Sigma), and 100 μg/mL normocin (InvivoGen) (cRPMI) and kept at 3-6x10^5 cells/mL in culture. Jurkat T cells (3x10^6) were transfected with 2 μg of respective A20 expression plasmid DNA, except the N-term fragment (0.5 μg). Transfections were performed using a BTX Electroporator (BTX Harvard Apparatus: 260 V, 950 μF) in 400 μL antibiotic-free RPMI 1640 medium supplemented with 10% FBS and rested for 24 hours prior to subsequent experiments. When performing NF-κB and AP-1 reporter assays, cells were simultaneously co-transfected with 2 μg of either reporter plasmid/3x10^6 cells.

Stimulation reagents and conditions

Reagents used for Jurkat T cell and human primary T cell stimulation experiments include anti-human CD3 (BD; HIT3α), anti-human CD28 (BD, CD28.2), phorbol 12-myristate 13-acetate (PMA; Cayman), ionomycin (Sigma), and anti-CD3/anti-CD28-conjugated beads. PMA and ionomycin stocks were dissolved in DMSO. Anti-CD3/anti-CD28-conjugated beads were generated by coupling Dynabeads M-450 Epoxy beads (ThermoFisher) with anti-human CD3 and anti-human CD28 Abs [46]. For soluble antibody stimulation, anti-human CD3/CD28 were added to complete media at a final concentration of 1 μg/mL and mixed with cells. For plate-bound stimulation, wells of cell culture treated plates were coated with 1 μg/mL anti-human CD3 in phosphate buffered saline (PBS) at 4°C. Anti-human CD28 was added to complete media and mixed with cells at a final concentration of 1 μg/mL. For bead stimulation, anti-CD3/anti-CD28-conjugated beads were added at a 1:1 cell:bead ratio. For specific experiments using pharmacological inhibitors, cells were pre-incubated with 1 μM JNK Inhibitor 8 (JNK-IN-8; Millipore Sigma), 1 μM BI-605906 (IKKβ inhibitor; Cayman), 3 μM MALT1 inhibitor (MLT-748), or DMSO solvent (1:1000) for 1 hour prior to stimulation.

Primary human T cell isolation, generation of knockout primary human T cells, culture, and expansion

Buffy coats from healthy donors were generously provided by Dr. Michael Lenardo and the National Institutes of Health Blood Bank. Methods for primary T cell isolation, manipulation, and culture including: isolation of peripheral blood mononuclear cells (PBMC) using Ficoll gradient, purification of resting T cells from PBMC, activation, culture conditions, and preparations, quantifications, and data analysis for RICD assays were recently published [46]. In brief, on Day 0, peripheral blood mononuclear cells (PBMC) were isolated via Ficoll density centrifugation, and T cells were purified from PBMC using the EasySep Human T Cell Isolation Kit (Stem Cell Technologies). Purified T cells were rested at 1x10^7 cells/mL in antibiotic free RPMI 1640 for one hour at 37°C. Subsequently, A20 (*TNFAIP3*) knockout was performed via CRISPR-Cas9-based targeting, using the proprietary Alt-R platform from Integrated DNA

Technologies (IDT), with a protocol adapted from Seki and Rutz [47]. Pre-designed crRNA targeting *TNFAIP3* (A20) (5'-AACCATGCACCGATACACAC-3'), non-targeting (NT) crRNA (5'-CCATATCGGGGCGAGACATG-3') and tracrRNA were acquired from IDT and resuspended at 100 μM in RNase-free H_2O. For the generation of duplexes, crRNA and tracrRNA were mixed at a 1:1 ratio of crRNA:tracrRNA and incubated in a PCR thermocycler at 95°C for 5 minutes, followed by slowly cooling to 25°C. Ribonucleoprotein (RNP) complexes were prepared by mixing crRNA/tracrRNA duplexes with 61 pmol/uL Alt-R *S. pyogenes* Cas9 Nuclease V3 (IDT) at a 3:1 ratio for 10 minutes at room temperature. Subsequently, $1x10^7$ human T cells were resuspended in 40 μL primary cell nucleofection solution (P3 Primary Cell 4D-Nucleofector X Kit, Lonza) and mixed with 15 μL of RNP mixture. The cell/RNP mixture was transferred to nucleofection cuvettes and electroporated with a 4D-Nucleofector (Lonza) using the EH100 program. Nucleofected cells were then immediately transferred to antibiotic free RPMI 1640 medium supplemented with 10% FBS in 6 well plates and incubated at 37°C. On Day 2, cells were resuspended at $2x10^6$ cells/mL in RPMI 1640 medium supplemented with 1% penicillin-streptomycin and 10% FBS (complete RPMI 1640) and activated for 3 days with anti-CD3/anti-CD28-conjugated beads at a 1:1 cell:bead ratio. On Day 5, a magnet was used to remove the beads and activated T cells were cultured in cRPMI supplemented with 100 IU/mL recombinant human IL-2 (r-hIL-2; Peprotech) at 1-$1.5x10^6$ cells/mL, and maintained for up to 25 days. On Day 10, deletion of A20 was confirmed by immunoblotting, and experiments with primary human T cells were performed between Days 15-25.

Primary human T cell experiments

To confirm signaling defects in CRISPR/Cas9 RNP-edited primary human T cells, activated non-targeting (NT) and A20 KO effector T cells were resuspended in cRPMI without IL-2 at 2.4 million cells/ml in 24 well plates and left unstimulated or stimulated for 4, 6, 8 or 24 hours with 1 μg/mL of soluble anti-CD3/CD28 Abs or 20 ng/mL PMA and 1 μg/mL ionomycin. Lysates were collected from each time point and analyzed via immunoblotting.

To examine surface activation markers, activated NT and A20 KO effector T cells were left unstimulated or stimulated for 24 hours with 100 ng/mL anti-human CD3 (BioGems; OKT3), 1 μg/mL of anti-CD3/CD28 Abs, or 20 ng/mL PMA and 1 μg/mL ionomycin. Cells were washed and stained with PE-conjugated anti-human CD25 or PE anti-human CD69 Abs (BioLegend) and analyzed on an Accuri C6 Plus flow cytometer (BD). To assess the ratio of CD4:CD8+ T cells, cells were washed and surface stained with FITC anti-human CD4 antibody and APC anti-human CD8 antibody (BioLegend) and analyzed on an Accuri C6+.

To profile cytokine secretion, NT and A20 KO activated T cells were washed 2x with PBS to remove r-hIL-2 and rested in cRPMI for 24 hours. Subsequently, T cells were seeded at $2x10^6$ cells/mL and left unstimulated or stimulated with 1 μg/mL of anti-CD3/CD28 Abs or 20 ng/mL PMA and 1 μg/mL ionomycin. Supernatants were collected after 24 hours and stored at −80°C. Cytokine levels were assayed using the LEGENDplex Human Th Cytokine Panel kit (BioLegend) on an Accuri C6+ flow cytometer, according to the manufacturer's instructions.

For intracellular flow cytometry, samples were plated at $1x10^6$ cells/mL in cRPMI stimulated with 20 ng/mL PMA and 1 μg/mL ionomycin for 6 hours. At 6 hours, stimulation was halted by placing cells on ice and adding 1 mL of ice-cold PBS to each sample. Cells were then spun down in 2 mL tubes, resuspended in 200 μL of PBS, and plated onto a polypropylene 96-well U-bottom plate (Thermo Fisher). Plates were centrifuged at 1500 rpm for 5 minutes, supernatants were removed by flicking, and cells were resuspended in 100 μL of Zombie NIR (BioLegend) and kept in the dark at room temperature for 15 minutes. Cells were then washed as before and resuspended in 50 μL of surface staining master mix. Cells were stained with BV421 anti-CD3 (BioLegend), BUV496 anti-CD4 (BioLegend), and BUV805 anti-CD8 Abs (BioLegend) in a 50:50 mix of FACS Buffer (98.8% PBS, 1% FBS, and 0.2% Sodium Azide) and Brilliant Staining Buffer (BD Biosciences), on ice in the dark for 30 minutes. After surface staining, cells were washed as before and resuspended in 100 μL True-Nuclear Fixation Buffer (BioLegend) and incubated in the dark at room temperature for 1 hour. After centrifugation at 1500μL for 5 minutes, cell pellets were resuspended with 50μL of intracellular staining mix: PE/Cy7 anti-PU.1, Alexa Fluor 488 anti-FOXP3, BV785 anti-TBET, Alexa Fluor 647 anti-GATA3 Abs (BioLegend) and PE anti-RORγT (BD Biosciences) in a 50:50 mix of Permeabilization Buffer from the True-Nuclear Fixation Buffer Kit and Brilliant Staining Buffer. Cells were incubated in staining mix at room temperature, in the dark, for 40 minutes. Cells were then washed with Permeabilization buffer, and then resuspended in 200 μL into flow cytometry tubes. Cell samples were analyzed on a 5-laser Cytek Aurora. Analysis of flow cytometry data was done on FlowJo software. All flow cytometry experiments adhered to appropriate guidelines for immunological studies [48].

To examine how A20 deletion impacts apoptosis sensitivity, we employed multiple flow cytometric techniques including AnnexinV staining, propidium iodide (PI) exclusion, and PI cell cycle analysis [49]. T cell apoptosis was measured by staining with APC AnnexinV (BioLegend) and propidium iodide (ThermoFisher) to identify early and late apoptotic cells. For PI cell cycle analysis, stimulated T cells ($0.5x10^6$) were washed 1x in PBS and stained with 0.5 ml of buffer containing 50 mg/ml PI, 0.1% Triton X-100, 1 mg/ml sodium citrate, and 1 mg/ml RNAse A (Sigma). Relative DNA content for distinct cell phases (including subG1 apoptotic cells with fragmented DNA) was assessed by flow cytometry (Accuri C6+) after 18-24 hrs of anti-CD3 (OKT3) or 200 nM staurosporine (STS) restimulation. RICD assays were performed as previously described [46]. Briefly, activated T cells were treated in triplicate with 100 ng/mL of anti-human CD3 (BioGems; OKT3) and plated at $2x10^5$ cells/well in 96-well round bottom plates. For some assays, cells were pretreated for 1 hour with 1 μM JNK and/or IKKβ inhibitors (JNK-IN-8 or BI-605906, respectively) or 200 nM staurosporine (STS). After 18-22 hours of TCR restimulation, cells were stained with PI at a final concentration of 1 μg/mL and collected for constant time (15-30 sec) on an Accuri C6+ flow cytometer (BD Biosciences). For CWID assays, NT and A20 KO activated T cells were washed 2x with PBS to remove r-hIL-2 and placed in complete RPMI 1640 medium. To inhibit IL-2, 1 μg/mL of anti-IL-2 (Mq1-17H12, eBiosciences) was added to complete media. Cells were then seeded at $2x10^5$ cells per well of a 96 well round bottom plate at 37°C. At 0, 24, 48, 72, and 96 hours post seeding, cells were stained with 1 μg/mL PI to quantify cell death by flow cytometry (Accuri C6+).

Statistical analysis

All statistical analyses were performed using GraphPad Prism (v10). For in vitro assays evaluating differences between treatments and genotypes (AP-1- and NF-κB-driven GFP reporters), ordinary one-way ANOVAs with Dunnett's multiple comparison tests were used, except when inhibitors were included, for which unpaired t-tests were utilized as described in figure legends. Relative expression of A20 fragments was compared with ordinary one-way ANOVAs and Dunnett's multiple comparison tests. To compare NT and A20 KO primary human T cells, a paired t-test was used. Differences between mean values were considered significant when $p < 0.05$ for all experiments, and significance is indicated in each figure legend.

RESULTS

A20 is a negative regulator of CBM-dependent pathways following T-cell receptor stimulation.

To investigate A20 as a negative regulator of TCR stimulation, we utilized wild-type (WT) and A20 knockout (KO) Jurkat T cell lines transfected with an empty vector (EV) or WT A20 expression vector (Figure 1A), titrated to approximate endogenous A20 expression in WT Jurkat (Figure S1A). We first examined NF-κB signaling utilizing immunoblots and a co-transfected NF-κB-driven GFP reporter. In response to PMA/ionomycin stimulation, we observed sustained IκBα degradation over 4 hours in A20 KO Jurkat cells relative to WT Jurkat (Figure 1B). Normal IκBα degradation and re-expression was restored upon complementation with a dual Myc/FLAG-tagged WT A20 construct (Figure 1B). Utilizing the GFP reporter, we confirmed heightened NF-κB activity in A20 KO Jurkat cells after PMA/ionomycin stimulation relative to WT cells, which was reversed by ectopic restoration of WT A20 expression (Figure 1C). Similar results were obtained after stimulation with anti-CD3/CD28 antibodies (Figure 1C, S1B) with excess NF-κB activity suppressed by complementation with WT A20 with or without N-terminal Myc or C-terminal FLAG tags included (Figure S1C).

Early studies connected CARD11 to JNK2 activation [50], and our group recently illuminated the importance of CARD11 in facilitating the activation of both JNK1 and JNK2 in T cells (Bauman, in review). Although A20 has been linked to JNK regulation in other cell types, the effect of A20 on CBM-dependent JNK signaling has yet to be examined after acute T cell stimulation. Remarkably, deletion of A20 also led to sustained JNK phosphorylation, as well as enhanced phosphorylation and accumulation of c-Jun over time (Figure 1D). Similar to NF-κB signaling, ectopic A20 complementation reversed these effects. Considering c-Jun is a component of canonical AP-1/c-Fos heterodimers, we also assessed whether AP-1-dependent transcription was impacted by A20 loss utilizing a co-transfected AP-1 driven GFP reporter plasmid containing repeat c-Jun/c-Fos consensus binding sites capable of reporting the activity of multiple AP-1 dimers. We measured a significant increase in AP-1 activity in A20 KO cells post-stimulation; introduction of WT A20 protein restored AP-1 activity to levels comparable to WT Jurkat cells (Figure 1E). Upon pre-treating cells with a specific JNK inhibitor (JNK-IN-8), we confirmed the increase in AP-1 activity in A20 KO cells was due to increased CBM-dependent JNK signaling

(Figure 1F). Our findings demonstrate that A20 regulates both NF-κB *and* JNK signaling downstream of the CBM complex after TCR/CD28 ligation.

A20 domains differentially regulate NF-κB and JNK in following T cell stimulation.

We next dissected the importance of distinct A20 protein domains in modulating NF-κB and JNK signaling by employing a set of novel, dual Myc/FLAG-tagged A20 variant constructs (Figure 2A). These expression vectors included both full-length WT A20 as well as N-and C-terminal fragments produced after MALT1-mediated proteolytic cleavage triggered post-TCR engagement [3]. Additional missense mutations were introduced to disrupt specific functional domains as referenced below. A non-cleavable A20 construct was also produced in which the MALT1-dependent cleavage site is mutated (p.Arg439Ala, R439A) [36]. To test the role of critical A20 ZnF domains, ZnF4 was mutated to abolish E3 ligase activity (mZnF4: C609A/C612A) and ZnF7 was mutated to disrupt the M1-linear ubiquitin binding site (mZnF7: C764A/C767A) [3, 37, 39, 40, 51, 52]. Similarly, the OTU domain was mutated to inactivate deubiquitinase (DUB) activity (mDUB : C103A) [2, 3, 35, 37–39]. The expression of each mutant protein in transfected A20 KO Jurkat cells was confirmed by immunoblotting, and constructs were titrated to approximate endogenous levels of expression of WT A20 (Figure S2A). Utilizing the same NF-κB-driven GFP reporter assay, we found that preventing M1-linked ubiquitin binding through ZnF7 (mZnF7) completely abrogated the ability of A20 to negatively regulate NF-κB compared to WT (Figure 2B). Similarly, removal of ZnF4-mediated E3 ligase activity (mZnF4) reduced A20-dependent NF-κB regulation, although this effect did not reach statistical significance relative to WT (Figure 2B). By contrast, the DUB function of A20 was indeed dispensable for NF-κB regulation (mDUB), matching recent reports (Figure 2B) [27]. Similarly, neither N- nor C-terminal fragments retained the ability to blunt NF-κB when expressed individually (Figure 2B). These results were consistent with previous work that showed co-transfection of both N- and C-terminal fragments together cannot compensate for full length A20 and does not dampen NF-κB [36]. To interrogate whether these structural domains conferred A20 functional activity beyond currently defined enzymatic activities, we also made constructs with ZnF4, ZnF7, or OTU domains deleted entirely (ΔZnF4, ΔZnF7, ΔOTU). Loss of any of these domains completely abrogated regulatory function, suggesting each is required to maintain A20 protein structure and function (Figure 2C). Effects of each A20 mutant on NF-κB activity persisted over time after PMA and ionomycin stimulation, with significant differences noted out to 24 hours even as overall levels of NF-κB activation largely subsided (Figure S2B).

Utilizing the AP-1 driven GFP reporter in our A20 KO transfection system, we found similar effects with each A20 mutant construct to those observed for NF-κB activity (Figure 2C). Both noncleavable and mDUB A20 were able to negatively regulate AP-1 activity similar to WT, congruent with effects on NF-κB activity (Figure 2D). Conversely, both ZnF4 and ZnF7 appeared to be necessary for AP-1 regulation, mirroring the pattern for NF-κB regulation and implying that A20 is primarily acting on the CBM signalosome upstream of both pathways (Figure 2D).

To assess if individual A20 mutants were able to directly engage active components within the CBM complex, we measured MALT1-dependent cleavage by immunoblotting as a surrogate for A20-MALT1 colocalization, as recently described [27]. By utilizing A20 KO Jurkat cells transfected with dual-tagged A20 mutant constructs, the generation of A20 cleavage products was tracked via immunoblot of N-terminal (Myc) or C-terminal (FLAG) tagged fragments 4 hours post-stimulation, with or without pre-treatment with a MALT1 protease inhibitor (MLT-748) (Figure 3). As expected, WT A20 was cleaved upon stimulation and the non-cleavable A20 was not. In contrast to WT, mutation of the ZnF7 active site completely abrogated MALT1-dependent A20 cleavage after TCR stimulation, suggesting that ZnF7 helps localize A20 to the CBM complex via linear ubiquitin binding (Figure 3) [13, 39]. Moreover, complete deletion of ZnF4, ZnF7, or OTU domains also abrogated MALT1 cleavage of A20. By contrast, mDUB and mZnF4 A20 proteins were cleaved to a similar extent as WT A20, suggesting the catalytic activity of these domains is dispensible for A20 localization to the CBM complex. Importantly, MALT1 mutant cleavage patterns were congruent with their functional effects in NF-κB and AP-1 reporter experiments (Figure 2A–B). In summation, ZnF7 appears particularly important in facilitating A20-dependent regulation of the CBM complex, evidenced by modulation of NF-κB- and JNK/AP-1-dependent transcription and MALT1 protease activity.

Loss of A20 in human primary effector T cells results in sustained NF-κB and JNK signaling and enhanced upregulation of activation markers.

To effectively delete A20 in primary, activated human T cells isolated from healthy donors, we utilized our recently reported CRISPR/Cas9 protocol [38]. These primary T cells were then expanded in IL-2 to derive effector T cells for various functional experiments (Figure 4A). Successful inactivation of the A20 gene was detected on Day 10, as evidenced by greatly reduced expression of A20 protein relative to non-targeted (NT) cells (Figure 4A). No difference was noted in the proportion of CD4+ to CD8+ cells between A20 KO and NT (Figure 4A, S3A). We first confirmed the same signal dysregulation that we observed in WT and A20 KO Jurkat T cells, noting a trend for enhanced acute NF-κB and JNK signaling readouts in A20 KO primary T cells by immunoblot, including prolonged IκBα degradation and sustained JNK phosphorylation and c-Jun accumulation (Figure 4B). We also observed a significant upregulation of CD69 and CD25 (IL-2Rα) in A20 KO cells versus NT upon restimulation, demonstrating enhanced AP-1- and NF-κB-dependent transcription, respectively (Figure 4C) [53, 54]. Although CD25 was already expressed on effector T cells as expected, A20 KO cells induced more cell surface CD25 expression versus NT after restimulation (Figure 4C, S3B). Intriguingly, these differences in activation marker upregulation were dependent on the stimulus utilized, with greater differences observed using soluble versus bead-conjugated anti-CD3/CD28 antibodies (Figure 4C). These results suggest a A20 is particularly important for preventing a mild to moderate TCR stimulus from inducing an excessive response, whereas strong stimulation overrides A20-dependent regulation [55, 56].

Increased cytokine secretion in A20 KO T cells

A recent report indicated that T cells derived from HA20 patients exhibited evidence of enhanced Th9/Th17 differentiation when cultured in polarizing conditions [14], with

elevated IL-17 and IL-9 production noted in HA20 patient sera and from stimulated PBMCs [3]. To investigate intrinsic differences in cytokine secretion when A20 is deleted in healthy donor T cells, we employed a bead-based multiplex assay to assess expression of twelve different cytokines by flow cytometry. After restimulation with PMA and ionomycin, most measured cytokines except IL-10 showed significantly increased production from A20 KO compared to NT T cells, including a trend for enhanced IL-5 and IL-17F production (Figure 5A). Similar results were obtained after restimulation with soluble anti-CD3/CD28 Abs, although some cytokines were too low to quantify accurately (Figure 5A). Even after substantial dilution of supernatants, IFN-γ levels consistently exceeded the detection limit with PMA and ionomycin stimulation, likely due to a very strong response from both CD8 and CD4 T cells. When plotted as a fold-change, we noted the largest relative increase in IL-9 produced by A20 KO cells relative to NT, congruent with enhanced Th9 skewing observed in HA20 patients [14]. Interestingly, A20 KO T cells also produced more Th2 cytokines (IL-4/13); indeed, Th2 cells can also produce IL-9, and IL-4 is known to promote Th9 differentiation via STAT6 signaling [57, 58]. Similar to HA20 patients, we also observed evidence of enhanced Th17 differentiation in A20 KO effector T cells, which produced more IL-6, IL-22, and IL-17A/F (Figure 5B). Our data suggest that in the absence of A20, dysregulated NF-κB and JNK signaling in T cells drives elevated production of multiple pro-inflammatory cytokines, and may predispose to enhanced Th9/Th17/Th22 differentiation in a T cell-intrinsic manner.

We also assessed expression of several relevant lineage specific transcription factors in WT and A20 KO effector T cells using intracellular flow cytometry. Gating on CD4+ T cells, we observed a statistically significant increase in the upregulation of RORγT, TBET, and GATA3 after a 6 hour restimulation, with a modest increase in PU.1 expression (Figure 5C). Upregulation of PU.1 and RORγT continued to increase at 24 hours post-stimulation in A20 KO T cells, suggesting potential intrinsic skewing toward Th9/Th17 subset lineages (Sup. Fig 4). Interestingly, similar results were obtained in CD8+ A20 KO T cells, highlighting a strong de-regulation of global cytokine expression when A20 is deleted, regardless of T cell lineage (Figure 5C).

Loss of A20 in human primary effector T cells results in decreased sensitivity to RICD and increases sensitivity to CWID.

In the context of infection, two distinct apoptosis programs regulate the expansion and contraction of effector T cells populations: restimulation induced cell death (RICD) and cytokine withdrawal induced death (CWID) [46, 59]. Both programs are critical for preventing collateral damage to host tissues and shaping a small T cell memory pool for effective recall responses. To examine how A20 deletion impacts apoptosis sensitivity, we employed multiple flow cytometric techniques including AnnexinV staining, propidium iodide exclusion, and PI cell cycle analysis. Upon TCR restimulation with OKT3, A20 KO T cells exhibited less AnnexinV staining compared to NT cells as an early indicator of reduced RICD (Figure 6A). This correlated with a decreased proportion of A20 KO cells in the subG1 phase of the cell cycle, which contains apoptotic cells undergoing DNA fragmentation (Figure 6B). We also observed an increased proportion of A20 KO cells in the S and G2/M phases, representing active DNA replication and cell division, respectively

(Figure 6B). These results suggest that, relative to NT, A20 KO effector T cells exhibit an increased proportion of actively cycling cells and a reduced proportion of cells undergoing apoptosis upon TCR restimulation. We also performed conventional RICD assays in which both NT and A20 KO T cells were restimulated with OKT3 for 24 hours, with % viable cells quantified by flow cytometry based on PI exclusion. We observed a trend towards greater viability in A20 KO T cells relative to NT for six of nine donors tested, although it did not reach statistical significance (Figure 6C). Similar results were obtained in response to the potent apoptosis inducer staurosporine (STS), which likely acts independently of A20/NF-κB function. (Figure 6C). However, when these cells were pre-treated with JNK and/or NF-κB inhibitors prior to TCR restimulation, we observed a significant decrease in cell viability with NF-κB inhibition (Figure 6D), consistent with a pro-survival advantage conferred by enhanced activity of this transcription factor family [60]. In culture, A20 KO cells consistently showed increased proliferation relative to NT based on cell counting, with more lactic acid produced to indicate increased metabolic activity (data not shown). Conversely, A20 KO cells appeared slightly more sensitive to CWID induced by IL-2 deprivation over 4 days in culture, which was further exacerbated by treatment with an IL-2 neutralizing Ab (Supp Fig 6). Taken together, these data suggest that elevated TCR-induced NF-κB activation in the absence of A20 renders effector T cells more proliferative and less susceptible to RICD. By contrast, A20-deficient T cells may die more quickly upon IL-2 withdrawal without TCR restimulation.

DISCUSSION

A20 is a ubiquitously expressed modulator of inflammatory signaling pathways throughout the body. Although mechanistic details remain unclear, the importance of A20 as a negative regulator of TCR-driven CBM-dependent NF-κB activation is well established. However, less is known regarding how A20-dependent regulation of crucial transcription factors downstream of the CBM complex impacts effector T cell function. Here, we highlight a novel role for A20 as a critical negative regulator of NF-κB *and* JNK/AP-1 signaling post-TCR stimulation, noting increased, sustained phosphorylation and accumulation of both JNK and c-Jun in A20 KO T cells. Additionally, using a novel AP-1-driven GFP reporter, we demonstrated a substantial JNK-dependent increase in AP-1-mediated transcription in A20 KO Jurkat cells, highlighting a novel function for A20 for modulating this CBM-dependent signaling pathway. Although we observed robust differences with mitogenic stimuli, signaling differences in CD4+ versus CD8+ T cells may be possible with antigen-specific stimulation.

Although A20 has been a known negative regulator of TCR cell signaling for a decade, the importance of distinct A20 protein domains in this process has remained confusing. Previously, A20 function was tested primarily in HEK293T cells or in cell-free contexts, with limited studies utilizing T cell lines or primary human T cells [2, 3, 36–38]. One recent study demonstrated augmented IL-2 and TNF secretion from primary human CD4+ T cells in which A20 or ABIN-1 were deleted [27]. Using A20 KO Jurkat cells complemented with a suite of mutant expression constructs and GFP reporters, we showed that the M1-ubiquitin binding domain ZnF7 is crucial for localization to and regulation the CBM complex; mutation or deletion of this domain abolished MALT1-dependent A20 cleavage

and enhanced both NF-κB and AP-1 activity. We also found that A20-dependent regulation is partially dependent on the ZnF4 domain, noting slight increases in NF-κB and AP-1 transcription and a modest decrease in MALT1-dependent cleavage of mZnF4/as compared to WT A20. Although A20 was reported to be capable of removing K63-Ub from MALT1 in a cell-free context [35], our data confirmed recent reports that A20 DUB activity is entirely dispensable for negative regulation of NF-κB activity in T cells [27, 36, 38], as well as AP-1 activity. Indeed, a recent report summarizing HA20 patient mutations and clinical severity highlighted that those harboring ZnF domain mutations (versus OTU variants) presented earlier in life with an increased proportion of patients developing musculoskeletal disorders [18]. To further develop a mechanistic understanding of the underlying biology, future studies should examine both A20 mRNA and protein expression across various cell types from HA20 patients to determine if specific mutations result in stable but non-functional protein expression.

Although the ubiquitin-editing function of A20 has been reported to target RIPK1, IKKγ/NEMO, and TRAF6 in the context of TNF signaling [3, 61], it remains unclear if/how these observations translate to TCR signaling through the CBM complex. Employing our ectopic expression system in Jurkat, we utilized MALT1-dependent cleavage as a surrogate for determining how domain variants impacted A20 interaction with the active CBM complex, mirroring results from a recent report [27]. Considering ZnF7 disruption had the most profound impact on downstream signaling (consistent with murine studies), a non-enzymatic mechanism for A20-dependent CBM regulation via binding to NEMO or other ubiquitinated partners is plausible [51, 62]. Notably, our extensive attempts to biochemically identify interactions between A20 and CBM partner proteins (including altered ubiquitination status) by co-immunoprecipitation were unsuccessful, perhaps due to the labile nature of the dynamic CBM signalosome in T cells. Future experiments might apply fluorescent microscopy or proximal ligation assays to better define how A20 dynamically interacts with the CBM complex post-TCR stimulation, alone or in concert with accessory proteins like ABIN-1 [27].

HA20 has been documented in 74 cases since its initial characterization in 2016, and the cohort continues to expand [14, 18, 63]. These patients suffer from systemic autoinflammatory disorders and are often diagnosed with BD [64]. Reports to date have largely focused on clinical presentation related to failed innate immune regulation. As noted in heterozygous A20 knockout mice, severe symptoms can be linked to overwhelming inflammation and excessive cell death triggered by cytokines (e.g. TNF, IL-1β) and/or pattern recognition receptors (e.g. TLR/NLRs) [2, 4, 7, 8, 14–17, 53–60]. Indeed, these symptoms can be alleviated by treatment with corticosteroids, disease modifying anti-rheumatic drugs (DMARDs) or biologics targeting TNF/IL-1β [14, 19, 63, 65, 66]. Nevertheless, these observations do not preclude a role for adaptive immune dysregulation in HA20 pathogenesis. However, few studies have focused on how HA20 patient T cell abnormalities might impact clinical disease [64, 67]. This prompted us to investigate the effects of A20 loss on primary human effector T cells by employing a powerful CRISPR/Cas9 RNP-based approach for highly efficient A20 deletion. Our results showed sustained TCR-induced NF-κB *and* JNK signaling over time in A20 KO primary T cells, mirroring our results in Jurkat lines. Moreover, we noted increased CD25 and CD69 expression in A20

KO T cells across multiple stimulation conditions, reflecting enhanced NF-κB and AP-1 activity, respectively [53, 54].

With regard to T cell effector function, one study found evidence of enhanced Th9/Th17 differentiation in HA20 patient T cells, with elevated IL-9 and IL-17 noted in HA20 patient sera and from stimulated PBMCs ex vivo [14]. These phenomena were largely attributed to extrinsic effects of excessive innate cytokine signaling on Th differentiation in vivo, with less focus on T cell intrinsic effects of A20 removal. Using a multiplex bead-based flow cytometric assay to assess expression of 12 different cytokines, we documented marked increases in the production of all measured cytokines except IL-10 post-stimulation in purified NT vs. A20-deleted bulk T cells. These results indicate an intrinsic global de-regulation of cytokine secretion when A20 is absent. Indeed, lineage-specific transcription factors were upregulated in both CD4+ and CD8+ A20 KO effector T cells upon stimulation (Figure 5C). However, evidence of some intrinsic CD4+ T cell skewing to Th9/17 fate may also help to explain specific phenotypes observed in HA20 and similar autoimmune conditions. Similar to HA20 patient T cells, we observed a substantial increase in IL-6, TNF-α, Th17A/F and IL-22 (IL-17A) production by A20 KO T cells, which may drive Th17-related pathologies in HA20 and BD including ocular disease, retinal scarring, uveitis and arthritis [68, 69]. Arthritis was also linked to increased Th17 cells in $A20^{ZnF7/ZnF7}$ mice, with disease amelioration noted after delivery of IL-17A neutralizing antibodies [70]. Interestingly, crossing of $A20^{ZnF7/ZnF7}$ mice with $Rag1^{-/-}$ mice abrogated arthritis whereas a cross with μMT^{-} mice did not, indicating T cells were driving pathology in this model [70]. A20 is also a direct negative regulator of IL-1R and IL-17R signaling, which can further boost production of proinflammatory cytokines such as IL-6, IL-1β, and IL-17 if left unchecked [6, 71]. These hallmarks of HA20 patient disease may reflect intrinsic Th17/Th22 skewing due to intrinsically elevated IL-6 production, perpetuating a positive feedback loop [14, 27].

A20 KO effector T cells also secreted more Th9/Th2 cytokines (IL-9, IL-4, IL-5, and IL-13) post-stimulation relative to NT, with the most impressive fold change noted for IL-9 and IL-4. Indeed, HA20 patient T cells produced more IL-9 in vitro under polarizing conditions [14]. Th9 cells are induced by TGF-β and IL-4 signaling and perhaps derived through a Th2-dependent pathway; evidence suggests they can exacerbate Th2 cytokine production and drive pathology in asthma and allergic disease models [72]. As noted in HA20 T cells, we also observed upregulation of the Th9 master transcription factor PU.1 in A20 KO T cells [73, 74]. Although HA20 patients lack signs of overt Th2 skewing noted in other primary atopic disorders [14, 75], some present with allergic symptoms (e.g. asthma, atopic dermatitis) [76] that could be associated with increased Th9 cells. Although T cell differentiation is always influenced by innate responses and the resulting extracellular cytokine milieu, our data imply an intrinsic T cell differentiation abnormality in HA20 that calls for further clinical and mechanistic investigation. Intriguingly, the anti-inflammatory cytokine IL-10 was the only one we measured with reduced secretion from A20 KO T cells. Although the status of IL-10 producing Tregs has not been carefully studied in HA20 patients, silencing of A20 suppressed IL-10 expression in dendritic cells, consistent with decreased IL-10-secreting cells in BD patients [69, 77, 78]. Importantly, potential differences we observed in cytokine expression may also reflect altered reactivation of naïve

versus memory T cells in unfractionated healthy donor PBMC. To pinpoint A20-dependent alterations in Th *differentiation*, it would be informative to repeat experiments with purified naïve CD4+ T cells under polarizing conditions, provided technical limitations can be overcome. Nevertheless, our data highlight a hitherto unappreciated, T-cell intrinsic role for A20 in regulating effector T cell cytokine production even under non-polarizing conditions, which might prompt future studies to tailor specific therapies targeted at specific T cell subsets.

Depending on cell context, A20 has been shown to convey both pro- and anti-apoptotic functions. Both NF-κB and AP-1 are critical for lymphocyte survival and proliferation following antigen engagement; NF-κB in particular is linked to enhanced survival in B and T cells. Indeed, apoptosis resistance in lymphomas with constitutive NF-κB activity can be attributed to concomitant, often biallelic A20 loss-of-function mutations, with ectopic A20 expression inducing spontaneous death [25, 26]. Intriguingly, we have also observed constitutive MALT1-dependent proteolysis of A20 in apoptosis-resistant primary B cells from patients with B-cell Expansion with NF-κB and T cell Anergy (BENTA) disease, caused by germline heterozygous gain-of-function (GOF) CARD11 mutations capable of constitutive NF-κB stimulation [79]. To investigate A20 function in effector T cell survival, we investigated how A20 deletion impacted cell death sensitivity in two major apoptotic pathways (RICD and CWID). Upon TCR re-ligation, A20 KO effector T cells showed reduced AnnexinV staining and DNA fragmentation compared to NT, suggesting A20 KO T cells were modestly more resistant to RICD. We also noted increased proportions of A20 KO T cells in S and G2/M phases, consistent with enhanced proliferation and cell cycle progression. This might explain why we observed no difference in RICD sensitivity between NT and A20 KO T cells using our classic PI exclusion RICD assay, which is based on counting viable cells - relative cell loss can reflect increased apoptosis as well as decreased proliferation, cell cycle arrest or other forms of cell death (e.g. necroptosis) (39). However, when treated with an NF-κB inhibitor (-/+ JNK inhibition) prior to stimulation, A20 KO T cells did show increased sensitivity to RICD using this assay. In summation, we interpret these results to show that enhanced TCR-induced NF-κB stimulation in the absence of A20 confers modest RICD resistance in human effector T cells, consistent with a pro-survival function for NF-κB in lymphocytes. By contrast, slightly more A20 KO T cells died following IL-2 withdrawal as compared to NT, implying an increased reliance on IL-2 signaling for survival when antigen is scarce. This interesting dynamic parallels observations made in pathogen-infected mice with conditional A20 deletion in T cells. Upon challenge with *Listeria monocytogenes*, antigen-specific A20 KO $CD8^+$ T cells showed more rapid clonal expansion but accelerated contraction (and increased apoptosis) after clearance, consistent with reduced RICD sensitivity (i.e. more robust clonal expansion) but enhanced CWID. Relative RICD sensitivity is often inversely correlated with CWID sensitivity, as we have observed previously in SAP-deficient T cells from X-linked lymphoproliferative disease patients [80]. Although lymphocyte numbers appear grossly normal in HA20 patients, future mechanistic studies aimed at replicating and expanding these findings with HA20 patient T cells are certainly worthwhile.

In conclusion, our study provides conclusive evidence for an important T-cell intrinsic role for A20 in influencing T cell survival and effector function. Although more biochemical

studies are warranted, our results imply that A20 confers these functions by regulating both NF-κB and JNK/AP-1 activity downstream of the CBM complex, engaging this signalosome through ZnF7-dependent ubiquitin binding. Our work prompts further evaluation of how T cell abnormalities specifically impact pathogenesis in HA20 disease.

Supplementary Material

Refer to Web version on PubMed Central for supplementary material.

ACKNOWLEDGMENTS

We thank Dr. Michael Lenardo and the NIH Blood Bank for providing access to normal donor buffy coats. We thank Guido Falduto, Elizabeth Kairis and Daniella Schwartz at the University of Pittsburgh for experimental assistance and consultation regarding HA20 patients. We also thank Chou-Zen Giam, Marzena Pazgier, Robert Kortum, Daniel Krappmann, and members of the Snow laboratory for helpful feedback and discussions. The opinions and assertions expressed herein are those of the authors and are not to be construed as reflecting the views of the Uniformed Services University of the Health Sciences or the United States Department of Defense. This work was funded by grants to A.L.S. from the National Institutes of Health (1R35GM139619, 1R01AI168295).

DATA AVAILABILITY STATEMENT

Data are available upon reasonable request from the corresponding author.

REFERENCES

1. Malynn BA and Ma A, A20: A multifunctional tool for regulating immunity and preventing disease. Cell Immunol, 2019. 340: p. 103914. [PubMed: 31030956]
2. Boone DL, et al. , The ubiquitin-modifying enzyme A20 is required for termination of Toll-like receptor responses. Nat Immunol, 2004. 5(10): p. 1052–60. [PubMed: 15334086]
3. Wertz IE, et al. , De-ubiquitination and ubiquitin ligase domains of A20 downregulate NF-kappaB signalling. Nature, 2004. 430(7000): p. 694–9. [PubMed: 15258597]
4. Opipari AW Jr., et al. , The A20 zinc finger protein protects cells from tumor necrosis factor cytotoxicity. J Biol Chem, 1992. 267(18): p. 12424–7. [PubMed: 1618749]
5. Heyninck K, et al. , The zinc finger protein A20 inhibits TNF-induced NF-kappaB-dependent gene expression by interfering with an RIP- or TRAF2-mediated transactivation signal and directly binds to a novel NF-kappaB-inhibiting protein ABIN. J Cell Biol, 1999. 145(7): p. 1471–82. [PubMed: 10385526]
6. Heyninck K and Beyaert R, The cytokine-inducible zinc finger protein A20 inhibits IL-1-induced NF-kappaB activation at the level of TRAF6. FEBS Lett, 1999. 442(2–3): p. 147–50. [PubMed: 9928991]
7. Lee EG, et al. , Failure to regulate TNF-induced NF-kappaB and cell death responses in A20-deficient mice. Science, 2000. 289(5488): p. 2350–4. [PubMed: 11009421]
8. Hitotsumatsu O, et al. , The ubiquitin-editing enzyme A20 restricts nucleotide-binding oligomerization domain containing 2-triggered signals. Immunity, 2008. 28(3): p. 381–90. [PubMed: 18342009]
9. Turer EE, et al. , Homeostatic MyD88-dependent signals cause lethal inflamMation in the absence of A20. J Exp Med, 2008. 205(2): p. 451–64. [PubMed: 18268035]
10. Tavares RM, et al. , The ubiquitin modifying enzyme A20 restricts B cell survival and prevents autoimmunity. Immunity, 2010. 33(2): p. 181–91. [PubMed: 20705491]
11. Chu Y, et al. , B cells lacking the tumor suppressor TNFAIP3/A20 display impaired differentiation and hyperactivation and cause inflammation and autoimmunity in aged mice. Blood, 2011. 117(7): p. 2227–36. [PubMed: 21088135]

12. Bosanac I, et al. , Ubiquitin binding to A20 ZnF4 is required for modulation of NF-kappaB signaling. Mol Cell, 2010. 40(4): p. 548–57. [PubMed: 21095585]
13. Skaug B, et al. , Direct, noncatalytic mechanism of IKK inhibition by A20. Mol Cell, 2011. 44(4): p. 559–71. [PubMed: 22099304]
14. Zhou Q, et al. , Loss-of-function mutations in TNFAIP3 leading to A20 haploinsufficiency cause an early-onset autoinflammatory disease. Nat Genet, 2016. 48(1): p. 67–73. [PubMed: 26642243]
15. Franco-Jarava C, et al. , TNFAIP3 haploinsufficiency is the cause of autoinflammatory manifestations in a patient with a deletion of 13Mb on chromosome 6. Clin Immunol, 2018. 191: p. 44–51. [PubMed: 29572183]
16. Berteau F, et al. , Autosomic dominant familial Behcet disease and haploinsufficiency A20: A review of the literature. Autoimmun Rev, 2018. 17(8): p. 809–815. [PubMed: 29890348]
17. Aeschlimann FA, et al. , A20 haploinsufficiency (HA20): clinical phenotypes and disease course of patients with a newly recognised NF-kB-mediated autoinflammatory disease. Ann Rheum Dis, 2018. 77(5): p. 728–735. [PubMed: 29317407]
18. Chen Y, et al. , Association of Clinical Phenotypes in Haploinsufficiency A20 (HA20) With Disrupted Domains of A20. Front Immunol, 2020. 11: p. 574992. [PubMed: 33101300]
19. Karri U, et al. , The Complexity of Being A20: From Biological Functions to Genetic Associations. J Clin Immunol, 2024. 44(3): p. 76. [PubMed: 38451381]
20. Wang S, et al. , An enhancer element harboring variants associated with systemic lupus erythematosus engages the TNFAIP3 promoter to influence A20 expression. PLoS Genet, 2013. 9(9): p. e1003750. [PubMed: 24039598]
21. Wang S, et al. , TALEN-mediated enhancer knockout influences TNFAIP3 gene expression and mimics a molecular phenotype associated with systemic lupus erythematosus. Genes Immun, 2016. 17(3): p. 165–70. [PubMed: 26821284]
22. Adrianto I, et al. , Association of a functional variant downstream of TNFAIP3 with systemic lupus erythematosus. Nat Genet, 2011. 43(3): p. 253–8. [PubMed: 21336280]
23. Catrysse L, et al. , A20 in inflammation and autoimmunity. Trends Immunol, 2014. 35(1): p. 22–31. [PubMed: 24246475]
24. Hovelmeyer N, et al. , A20 deficiency in B cells enhances B-cell proliferation and results in the development of autoantibodies. Eur J Immunol, 2011. 41(3): p. 595–601. [PubMed: 21341261]
25. Compagno M, et al. , Mutations of multiple genes cause deregulation of NF-kappaB in diffuse large B-cell lymphoma. Nature, 2009. 459(7247): p. 717–21. [PubMed: 19412164]
26. Kato M, et al. , Frequent inactivation of A20 in B-cell lymphomas. Nature, 2009. 459(7247): p. 712–6. [PubMed: 19412163]
27. Yin H, et al. , A20 and ABIN-1 cooperate in balancing CBM complex-triggered NF-kappaB signaling in activated T cells. Cell Mol Life Sci, 2022. 79(2): p. 112. [PubMed: 35099607]
28. Giordano M, et al. , The tumor necrosis factor alpha-induced protein 3 (TNFAIP3, A20) imposes a brake on antitumor activity of CD8 T cells. Proc Natl Acad Sci U S A, 2014. 111(30): p. 11115–20. [PubMed: 25024217]
29. Verdeil G and Schmitt-Verhulst AM, Unleashing antitumor T-cell activation without ensuing autoimmunity: the case for A20-deletion in adoptive CD8(+) T-cell therapy. Oncoimmunology, 2014. 3(10): p. e958951. [PubMed: 25941582]
30. Bedsaul JR, et al. , Mechanistic impact of oligomer poisoning by dominant-negative CARD11 variants. iScience, 2022. 25(2): p. 103810. [PubMed: 35198875]
31. Lork M, Staal J, and Beyaert R, Ubiquitination and phosphorylation of the CARD11-BCL10-MALT1 signalosome in T cells. Cell Immunol, 2019. 340: p. 103877. [PubMed: 30514565]
32. Hayden MS and Ghosh S, Shared principles in NF-kappaB signaling. Cell, 2008. 132(3): p. 344–62. [PubMed: 18267068]
33. Gaide O, et al. , Carma1, a CARD-containing binding partner of Bcl10, induces Bcl10 phosphorylation and NF-kappaB activation. FEBS Lett, 2001. 496(2–3): p. 121–7. [PubMed: 11356195]
34. Yang K and Chi H, mTOR and metabolic pathways in T cell quiescence and functional activation. Semin Immunol, 2012. 24(6): p. 421–8. [PubMed: 23375549]

35. Duwel M, et al. , A20 negatively regulates T cell receptor signaling to NF-kappaB by cleaving Malt1 ubiquitin chains. J Immunol, 2009. 182(12): p. 7718–28. [PubMed: 19494296]
36. Coornaert B, et al. , T cell antigen receptor stimulation induces MALT1 paracaspase-mediated cleavage of the NF-kappaB inhibitor A20. Nat Immunol, 2008. 9(3): p. 263–71. [PubMed: 18223652]
37. Lu TT, et al. , Dimerization and ubiquitin mediated recruitment of A20, a complex deubiquitinating enzyme. Immunity, 2013. 38(5): p. 896–905. [PubMed: 23602765]
38. De A, et al. , The deubiquitinase activity of A20 is dispensable for NF-kappaB signaling. EMBO Rep, 2014. 15(7): p. 775–83. [PubMed: 24878851]
39. Tokunaga F, et al. , Specific recognition of linear polyubiquitin by A20 zinc finger 7 is involved in NF-kappaB regulation. EMBO J, 2012. 31(19): p. 3856–70. [PubMed: 23032187]
40. Verhelst K, et al. , A20 inhibits LUBAC-mediated NF-kappaB activation by binding linear polyubiquitin chains via its zinc finger 7. EMBO J, 2012. 31(19): p. 3845–55. [PubMed: 23032186]
41. Li L, et al. , Localization of A20 to a lysosome-associated compartment and its role in NFkappaB signaling. Biochim Biophys Acta, 2008. 1783(6): p. 1140–9. [PubMed: 18329387]
42. Ma CA, et al. , Germline hypomorphic CARD11 mutations in severe atopic disease. Nat Genet, 2017. 49(8): p. 1192–1201. [PubMed: 28628108]
43. Rios KE, et al. , CARD19 Interacts with Mitochondrial Contact Site and Cristae Organizing System Constituent Proteins and Regulates Cristae Morphology. Cells, 2022. 11(7).
44. Shagin DA, et al. , GFP-like proteins as ubiquitous metazoan superfamily: evolution of functional features and structural complexity. Mol Biol Evol, 2004. 21(5): p. 841–50. [PubMed: 14963095]
45. Angel P, et al. , Phorbol ester-inducible genes contain a common cis element recognized by a TPA-modulated trans-acting factor. Cell, 1987. 49(6): p. 729–39. [PubMed: 3034432]
46. Pohida K, et al. , Restimulation-Induced Cell Death (RICD): Methods for Modeling, Investigating, and Quantifying RICD Sensitivity in Primary Human T Cells via Flow Cytometric Analysis. Bio Protoc, 2022. 12(4): p. e4326.
47. Seki A and Rutz S, Optimized RNP transfection for highly efficient CRISPR/Cas9-mediated gene knockout in primary T cells. J Exp Med, 2018. 215(3): p. 985–997. [PubMed: 29436394]
48. Cossarizza A, et al. , Guidelines for the use of flow cytometry and cell sorting in immunological studies (third edition). Eur J Immunol, 2021. 51(12): p. 2708–3145. [PubMed: 34910301]
49. Voss K, et al. , FOXP3 protects conventional human T cells from premature restimulation-induced cell death. Cell Mol Immunol, 2021. 18(1): p. 194–205. [PubMed: 31659245]
50. Blonska M, et al. , The CARMA1-Bcl10 signaling complex selectively regulates JNK2 kinase in the T cell receptor-signaling pathway. Immunity, 2007. 26(1): p. 55–66. [PubMed: 17189706]
51. Martens A, et al. , Two distinct ubiquitin-binding motifs in A20 mediate its anti-inflammatory and cell-protective activities. Nat Immunol, 2020. 21(4): p. 381–387. [PubMed: 32205881]
52. Polykratis A, et al. , A20 prevents inflammasome-dependent arthritis by inhibiting macrophage necroptosis through its ZnF7 ubiquitin-binding domain. Nat Cell Biol, 2019. 21(6): p. 731–742. [PubMed: 31086261]
53. Ballard DW, et al. , HTLV-I tax induces cellular proteins that activate the kappa B element in the IL-2 receptor alpha gene. Science, 1988. 241(4873): p. 1652–5. [PubMed: 2843985]
54. Castellanos MC, et al. , Expression of the leukocyte early activation antigen CD69 is regulated by the transcription factor AP-1. J Immunol, 1997. 159(11): p. 5463–73. [PubMed: 9580241]
55. Fuhrmann F, et al. , Adequate immune response ensured by binary IL-2 and graded CD25 expression in a murine transfer model. Elife, 2016. 5.
56. Allison KA, et al. , Affinity and dose of TCR engagement yield proportional enhancer and gene activity in CD4+ T cells. Elife, 2016. 5.
57. Veldhoen M, et al. , Transforming growth factor-beta 'reprograms' the differentiation of T helper 2 cells and promotes an interleukin 9-producing subset. Nat Immunol, 2008. 9(12): p. 1341–6. [PubMed: 18931678]

58. Dardalhon V, et al. , IL-4 inhibits TGF-beta-induced Foxp3+ T cells and, together with TGF-beta, generates IL-9+ IL-10+ Foxp3(-) effector T cells. Nat Immunol, 2008. 9(12): p. 1347–55. [PubMed: 18997793]
59. Larsen SE, et al. , Differential cytokine withdrawal-induced death sensitivity of effector T cells derived from distinct human CD8(+) memory subsets. Cell Death Discov, 2017. 3: p. 17031. [PubMed: 28580175]
60. Wan YY and DeGregori J, The survival of antigen-stimulated T cells requires NFkappaB-mediated inhibition of p73 expression. Immunity, 2003. 18(3): p. 331–42. [PubMed: 12648451]
61. Mauro C, et al. , ABIN-1 binds to NEMO/IKKgamma and co-operates with A20 in inhibiting NF-kappaB. J Biol Chem, 2006. 281(27): p. 18482–8. [PubMed: 16684768]
62. Wertz IE, et al. , Phosphorylation and linear ubiquitin direct A20 inhibition of inflammation. Nature, 2015. 528(7582): p. 370–5. [PubMed: 26649818]
63. Kadowaki T, Kadowaki S, and Ohnishi H, A20 Haploinsufficiency in East Asia. Front Immunol, 2021. 12: p. 780689. [PubMed: 34899744]
64. Yu MP, et al. , Haploinsufficiency of A20 (HA20): updates on the genetics, phenotype, pathogenesis and treatment. World J Pediatr, 2020. 16(6): p. 575–584. [PubMed: 31587140]
65. Shigemura T, et al. , Novel heterozygous C243Y A20/TNFAIP3 gene mutation is responsible for chronic inflammation in autosomal-dominant Behcet's disease. RMD Open, 2016. 2(1): p. e000223. [PubMed: 27175295]
66. El Khouri E, et al. , A critical region of A20 unveiled by missense TNFAIP3 variations that lead to autoinflammation. Elife, 2023. 12.
67. Kadowaki S, et al. , Functional analysis of novel A20 variants in patients with atypical inflammatory diseases. Arthritis Res Ther, 2021. 23(1): p. 52. [PubMed: 33549127]
68. Hu J, et al. , A20 Inhibits Intraocular Inflammation in Mice by Regulating the Function of CD4+T Cells and RPE Cells. Front Immunol, 2020. 11: p. 603939. [PubMed: 33613524]
69. He Y, et al. , Decreased expression of A20 is associated with ocular Behcet's disease (BD) but not with Vogt-Koyanagi-Harada (VKH) disease. Br J Ophthalmol, 2018. 102(8): p. 1167–1172. [PubMed: 29699987]
70. Razani B, et al. , Non-catalytic ubiquitin binding by A20 prevents psoriatic arthritis-like disease and inflammation. Nat Immunol, 2020. 21(4): p. 422–433. [PubMed: 32205880]
71. Garg AV, et al. , The deubiquitinase A20 mediates feedback inhibition of interleukin-17 receptor signaling. Sci Signal, 2013. 6(278): p. ra44. [PubMed: 23737552]
72. Malik S and Awasthi A, Transcriptional Control of Th9 Cells: Role of Foxo1 in Interleukin-9 Induction. Front Immunol, 2018. 9: p. 995. [PubMed: 29867972]
73. Chang HC, et al. , The transcription factor PU.1 is required for the development of IL-9-producing T cells and allergic inflammation. Nat Immunol, 2010. 11(6): p. 527–34. [PubMed: 20431622]
74. Gerlach K, et al. , TH9 cells that express the transcription factor PU.1 drive T cell-mediated colitis via IL-9 receptor signaling in intestinal epithelial cells. Nat Immunol, 2014. 15(7): p. 676–86. [PubMed: 24908389]
75. Milner JD, Primary Atopic Disorders. Annu Rev Immunol, 2020. 38: p. 785–808. [PubMed: 32126183]
76. Schwartz DM, et al. , Systematic evaluation of nine monogenic autoinflammatory diseases reveals common and disease-specific correlations with allergy-associated features. Ann Rheum Dis, 2021. 80(6): p. 788–795. [PubMed: 33619160]
77. Direskeneli H, Fujita H, and Akdis CA, Regulation of TH17 and regulatory T cells in patients with Behcet disease. J Allergy Clin Immunol, 2011. 128(3): p. 665–6. [PubMed: 21878243]
78. Cosan F, et al. , Natural Killer Cell Subsets and Their Functional Activity in Behcet's Disease. Immunol Invest, 2017. 46(4): p. 419–432. [PubMed: 28388249]
79. Snow AL, et al. , Congenital B cell lymphocytosis explained by novel germline CARD11 mutations. J Exp Med, 2012. 209(12): p. 2247–61. [PubMed: 23129749]
80. Snow AL, et al. , Restimulation-induced apoptosis of T cells is impaired in patients with X-linked lymphoproliferative disease caused by SAP deficiency. J Clin Invest, 2009. 119(10): p. 2976–89. [PubMed: 19759517]

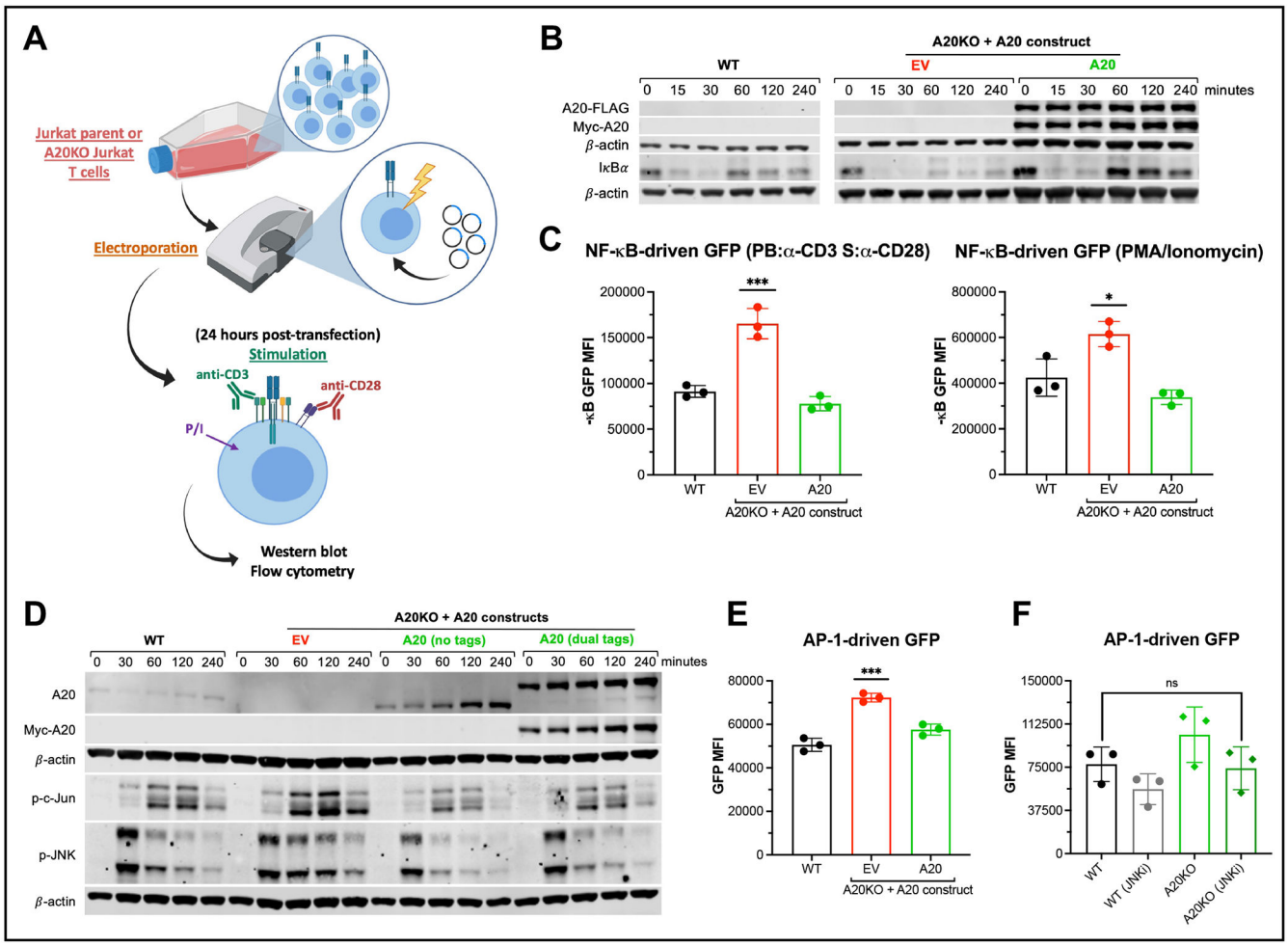

Figure 1. A20 is required to negatively regulate NF-κB and JNK signaling in Jurkat T cells.

(A) Schematic of transfection experimental design. **(B and D)** Wild-type (WT) or A20 KO Jurkat T cells were transfected with empty vector (EV) or **(B)** FLAG-Myc dual-tagged WT A20, or **(D)** untagged WT A20, and then stimulated 24 hrs later with 20 ng/mL PMA and 1 μg/mL ionomycin for 0-4 hours to simulate TCR-induced signaling. **(B)** NF-κB signaling was assessed by immunoblotting for IκBα degradation as a reliable and strong marker of NF-κB signaling. Representative immunoblot of 4 independent experiments. **(D)** JNK signaling was measured by immunoblotting for phosphorylation and accumulation of JNK and c-Jun. Representative immunoblot of 4 independent experiments. Cells transfected as in (A) plus an **(C)** NF-κB-driven GFP reporter or **(E-F)** an AP-1-driven GFP reporter construct were stimulated with 1 μg/mL of plate-bound anti-CD3 and soluble anti-CD28 agonistic Abs or 20 ng/mL PMA and 1 μg/mL ionomycin **(F)** in presence of 1 uM JNK-IN-8 inhibitor. GFP expression was measured by flow cytometry 6 hrs post-stimulation. GFP mean fluorescence intensity (MFI) represents a readout of NF-κB or AP-1-dependent transcriptional activity. Asterisks denote significance vs. WT Jurkat (one-way ANOVA, * $p<0.05$, *** $p < 0.001$; n=3, unpaired T test, ns>0.05, n=3). Data are representative of 3 independent experiments.

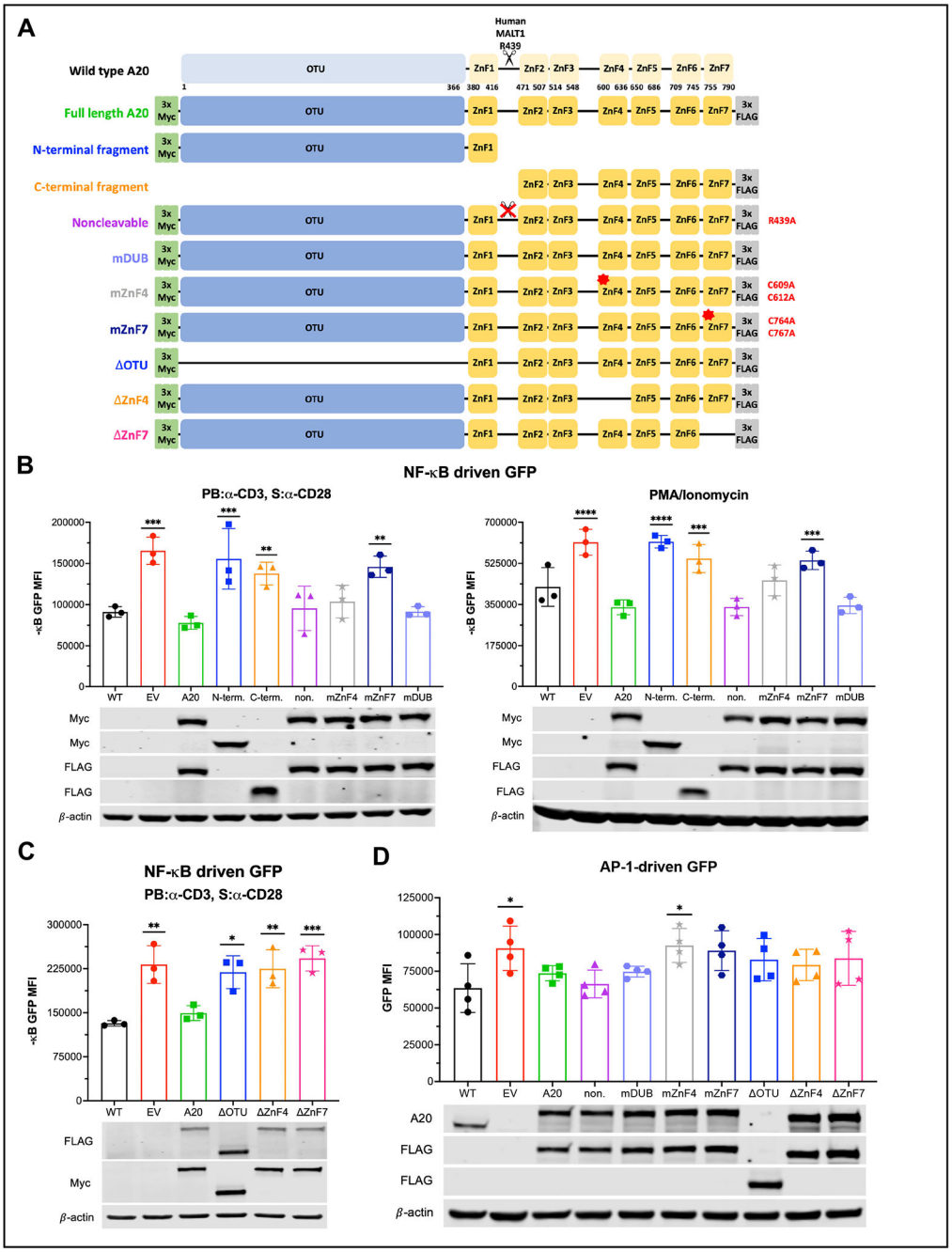

Figure 2: The DUB domain is dispensable, but ZnF4 and ZnF7 domains are required for A20-dependent NF-κB and JNK regulation.

(A) A20 expression constructs were cloned into a pUNO vector (InvivoGen), including full-length WT A20, N-and C-terminal fragments (normally generated after MALT1 cleavage), a non-cleavable A20 construct (R439A), mutants known to compromise ZnF4 E3 ligase activity (C609A/C612A), ZnF7 ubiquitin binding (C764A/C767A), and OTU domain deubiquitinase (DUB) activity (C103A), and complete deletions of OTU, ZnF4 and ZnF7 domains. All vectors include N-terminal 3x-Myc and C-terminal 3X-FLAG tags. **(B-D)** A20

KO Jurkat T cells were transfected with an (B-C) NF-κB-dependent GFP reporter or (D) AP-1-dependent GFP reporter construct plus A20 expression constructs or EV, and then stimulated with 1 μg/mL of plate-bound anti-CD3 and soluble anti-CD28 Abs or 20 ng/mL PMA and 1 μg/mL ionomycin to simulate TCR-induced signaling. GFP MFI was recorded by flow cytometry over a 24 hour period to monitor NF-κB-dependent transcription; data shown are (B-C) 6 hours or (D) 4 hours post-stimulation. Asterisks denote statistical significance vs. WT Jurkat (one-way ANOVA, *$p<0.05$, **$p < 0.01$; ***$p < 0.001$; ****$p < 0.0001$; n=3). Data are representative of (B-C) 3 or (D) 4 independent experiments.

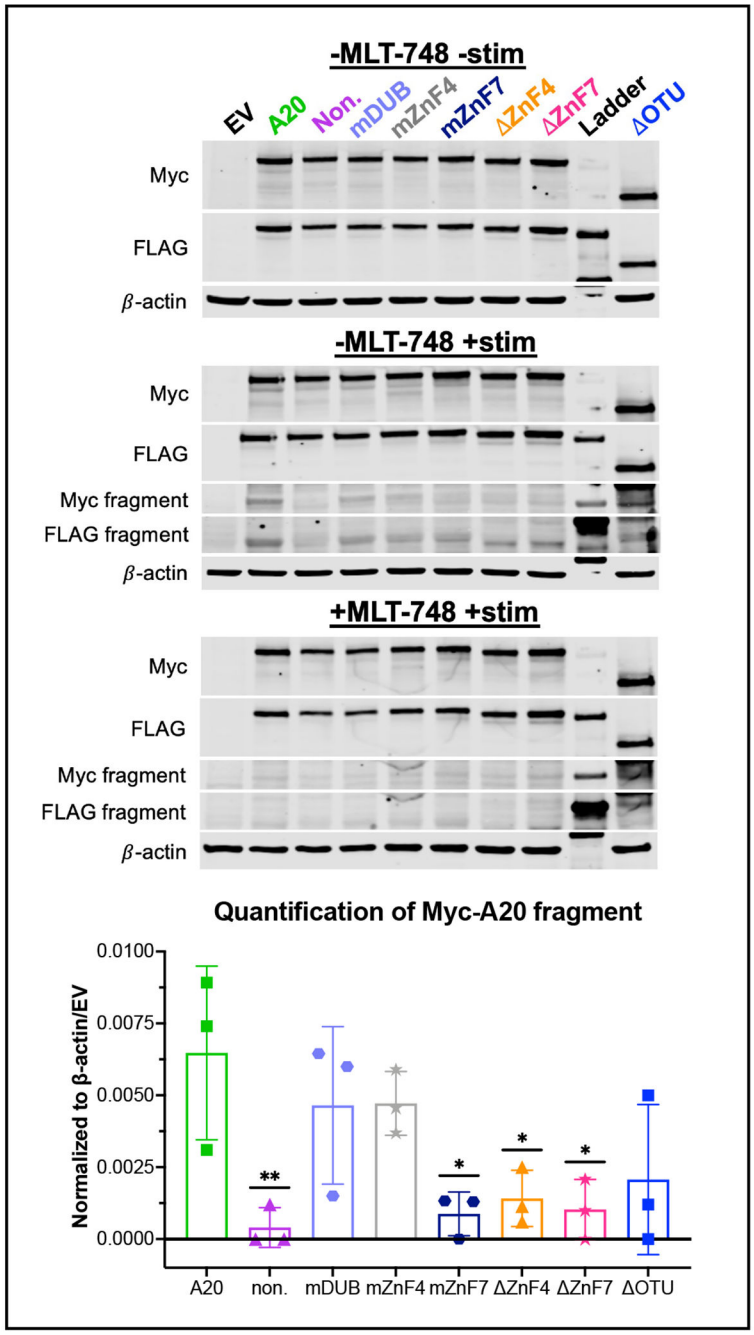

Figure 3: Localization of A20 to the CBM complex is dependent on ZnF7.

Relative generation of Myc-tagged N-terminal A20 fragment was quantified by spot densitometry, normalized to β-actin. Asterisks denote statistical significance vs. WT A20 transfectants (one-way ANOVA, *p<0.05, **p < 0.01 n=3). A20 KO Jurkat T cells were transfected with A20 expression constructs (Fig 2a) or EV. At 24hrs post-transfection, cells were pre-treated with DMSO or 10 nM of the MALT1 protease inhibitor MLT-748, and then stimulated with 20 ng/mL PMA and 1 μg/mL ionomycin for 4 hrs. As a surrogate for A20 colocalization with the active CBM complex, generation of MALT1-dependent cleavage

products was monitored by immunoblotting for N- (Myc) or C-terminal (FLAG) tagged fragments (middle panel, which were largely eliminated by MLT-748 pre-treatment (bottom panel). Untreated transfectants left unstimulated were utilized as a control (top panel). Data are representative of 3 independent experiments.

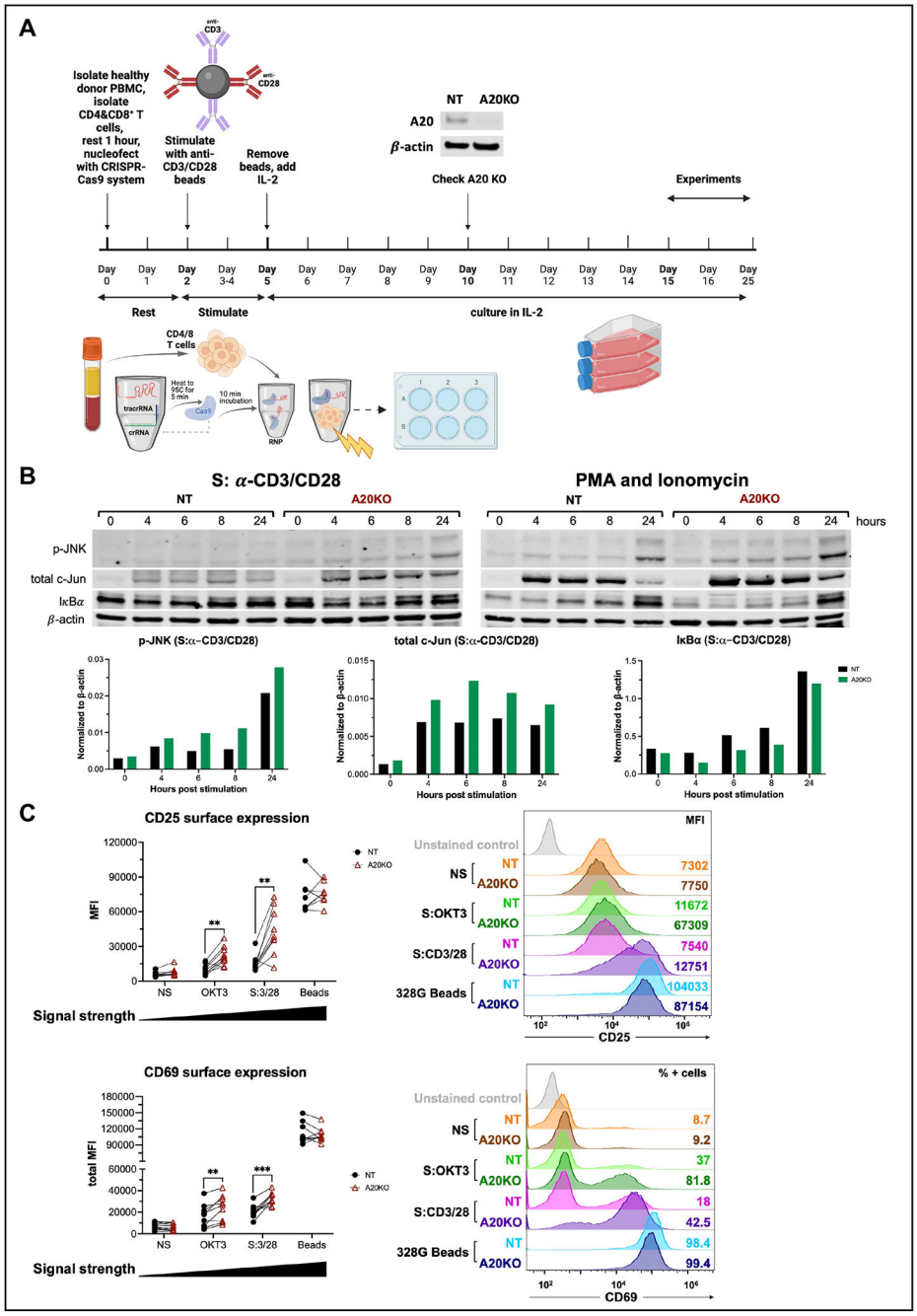

Figure 4. Loss of A20 in human primary effector T cells results in sustained NF-κB and JNK signaling and enhanced upregulation of activation markers.

(A) Generation of A20 knockout primary human effector T cells. Protocol timeline for generation of A20 knockout effector human T cells using Amaxa transfection of non-targeting (NT) or A20 gRNA-targeted CRISPR-Cas9 ribonucleoproteins. After 48 hrs, transfectants are stimulated for 3 days using anti-CD3/CD28 Ab-coupled beads, washed and cultured in 100U/ml rIL-2 for 15-25 days to generate effector T cells. A20 deletion is confirmed by immunoblotting lysates generated from day 10 effectors transfected with 5-10

ml (75-150 pmol) of crRNA-Cas9 RNP complexes. **(B)** NT and A20 KO effector T cells (donor 353, day 18) were stimulated with 1 μg/mL of anti-CD3/CD28 Abs or 20 ng/mL PMA and 1 μg/mL ionomycin. Lysates were collected from unstimulated cells (0) or at timepoints 4-24 hrs post-stimulation. Relative expression of phospho-JNK, c-Jun, and IkB was assessed by immunoblotting. Relative expression of proteins in were quantified by spot densitometry, normalized to β-actin and β-tubulin. Data are representative of 3 independent experiments using separate donors. **(C)** NT and A20 KO effector T cells (donor G4, day 18) were stimulated with 1 μg/mL of anti-CD3/CD28 Abs, 100 ng OKT3, or anti-CD3/CD28 Ab-coupled beads. CD69 and CD25 expression was assessed by flow cytometry at 24 post-stimulation; relative MFI is plotted per donor (right panel). Gating strategy is included in Figure S6A. Asterisks denote statistical significance WT vs. A20 KO (paired T-test, *$p<0.05$, **$p < 0.01$ n=9). Representative histogram of 9 independent experiments using separate donors.

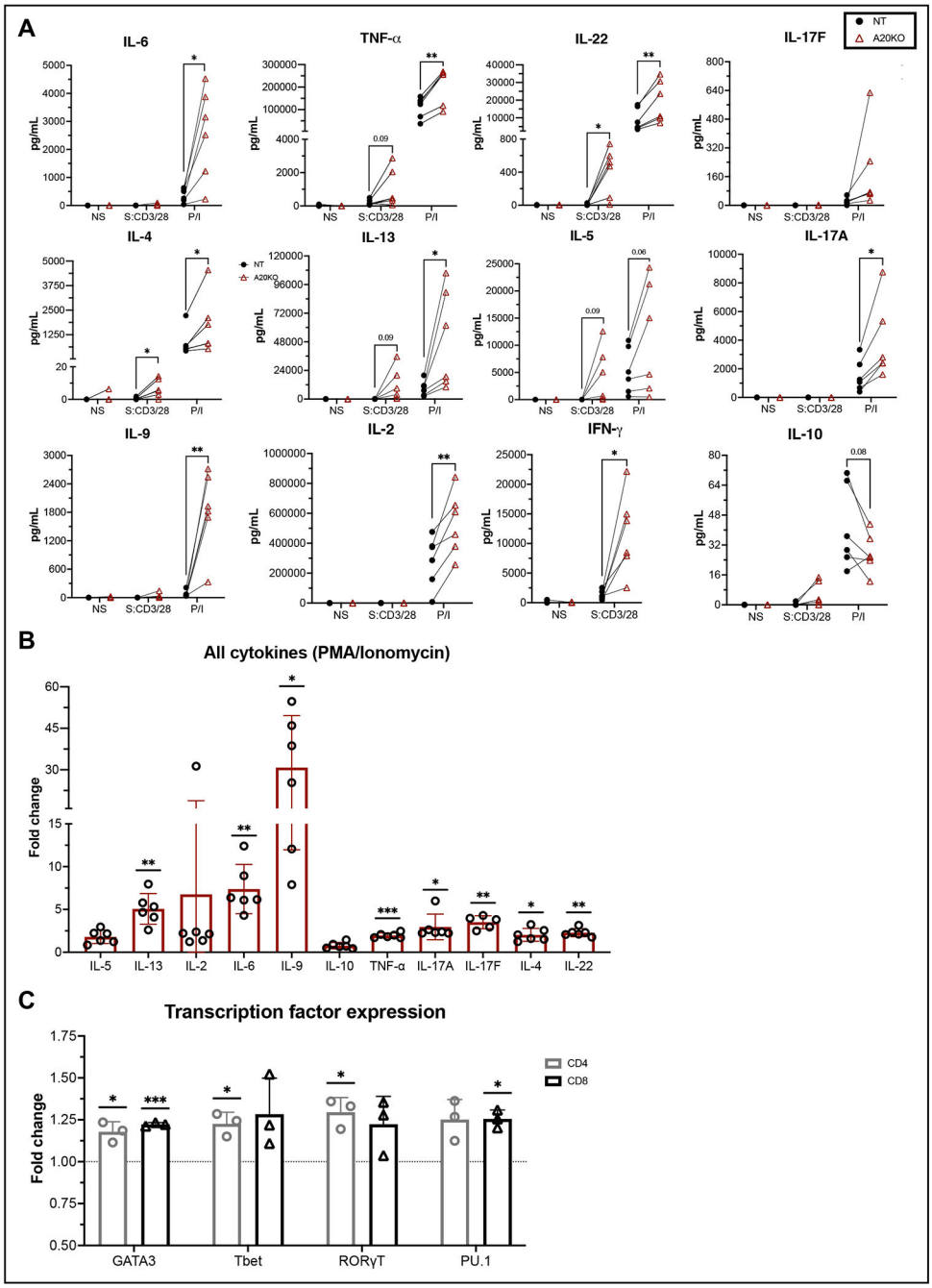

Figure 5. A20 KO T cells display elevated cytokine secretion.

(A) NT and A20 KO effector T cells were left unstimulated or stimulated for 24 hrs with 1 μg/mL of anti-CD3/CD28 Abs or 20 ng/mL PMA and 1 μg/mL ionomycin. Cytokine levels were measured in cell supernatants using the flow cytometric LEGENDPlex T Helper Cytokine Panel. **(B)** Fold change was quantified as the difference between A20 KO/NT predicted concentrations. **(C)** NT and A20 KO effector T cells were stimulated for 6 hours with 20 ng/mL PMA and 1 μg/mL ionomycin. Lineage transcription factors were measured by intracellular flow cytometry; gating strategy is included in Figure S6B. Fold change was

quantified as the difference between A20 KO/NT relative mean fluorescence intensity for CD4 and CD8 T cells. Asterisks denote statistical significance WT vs. A20 KO (paired T-test, *$p<0.05$, **$p < 0.01$, ***$p < 0.001$, n=6). Representative of 6 independent donors with 2 technical replicates per donor.

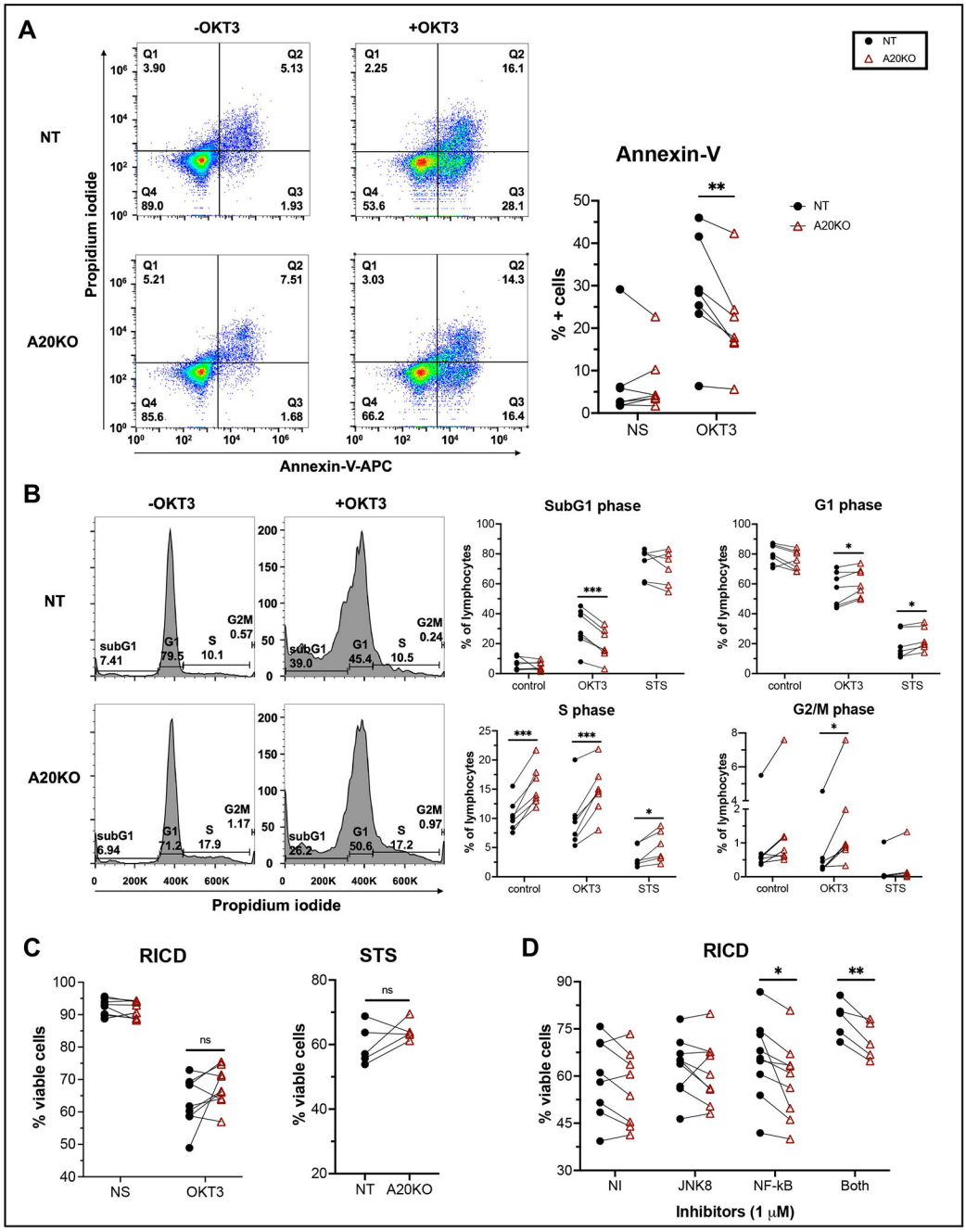

Figure 6. A20 KO T cells display decreased sensitivity to restimulation-induced cell death.

(A) NT and A20 KO effector T cells were stimulated for 24 hrs with 100 ng/ml anti-CD3 (OKT3), then stained to quantify cell death by flow cytometry with Annexin-V and propidium iodide [46]. Representative histogram of gating strategy of 7 independent experiments using separate donors. **(B)** PI cell cycle analysis was conducted and figures show the combination of the percentage of cells in each cell cycle stage from all 7 donors. **(C)** NT and A20 KO effector T cells were stimulated as in (A) and with 200 nM staurosporine, then stained with propidium iodide to quantify cell death by flow cytometry.

(D) RICD assay as performed in (A) after 1 hr pre-treatment with 1 uM of JNK inhibitor 8 (JNK8) and/or IKKβ inhibitor (NF-κB). Death assay data represent 5-9 independent donors. Asterisks denote statistical significance WT vs. A20 KO (paired T-test, *p<0.05, **p < 0.01, ***p < 0.001).

Table 1:

Primary antibodies used for immunoblot analysis and flow cytometry.

Supplier	Antibody Target	Clone	Catalog #
Cell Signaling	FLAG/DYKDDDDK Tag	9A3	8146
	Myc-tag	71D10	2278
	IκBα	L35A5	4814
	A20/TNFAIP3	D13H3	5630
	phospho-c-Jun (Ser63)	S4B3	2361
	phospho-SAPK/JNK (Thr183/Tyr185)	98F2	4671
	phospho-SAPK/JNK (Thr183/Tyr185)	G9	9255
	c-Jun	L70B11	2315
Biolegend	PE anti-human CD25 Antibody	M-A251	356104
	PE anti-human CD69 antibody	FN50	310906
	FITC anti-human CD4 antibody	RPA-T4	300538
	APC anti-human CD8 antibody	SK1	344722
	Zombie NIR	RUO	423111
	BV421 CD3	UCHT1	300433
	True-Nuclear Fixation Buffer	-	424401
	PE/Cyanine7 PU.1	7C6B05	658014
	BV785 T-bet	4B10	644835
	Alexa Fluor 647 GATA3	16E10A23	653810
	APC AnnexinV	-	640941
BD Biosciences	BUV496 CD4	GK1.5	612936
	BUV805 CD8	SK1	612889
	Brilliant Staining Buffer	-	563794
	PE RORγT	Q21-559	563081
ThermoFisher	anti-IL-2	MQ1-17H12	14-7029-81
	A20/TNFAIP3	59A426	MA5-16164
Sigma	β-actin	AC-15	A1978

Table 2.

Primer sequences used for molecular cloning and mutagenesis.

Primer Name	Primer Sequence (5’-3’)
3x MYC Amp Forward	CCGGCGCCTACCTGAGATCAACCGGTATGGCTAGTCTTAAAGAA
3x MYC Amp Reverse	GCCTGAGGAAGGACTTGTTCAGCCATGAATTCACTAGTAGTATG
A20 Amp Forward	ATGGCTGAACAAGTCCTTCCTCAG
A20 Amp Reverse	TCCGCCATACATCTGCTTGAACTGAAAG
3x FLAG Amp Forward	TCAAGCAGATGTATGGCGGAGAACGCGTGGACTACAAAGACCAT
3x FLAG Amp Reverse	ATCTTATCATGTCTGGCCAGGCGGCCGCCTACTTGTCATCGTC
Non-cleavable Forward	CTCGGGGCCTCTGCGGGAGAAGCCTAT
Non-cleavable Reverse	ATAGGCTTCTCCCGCAGAGGCCCCGAG
mZnF4 Forward	CAAGGGCTTTGCCACACTGGCTTTCATCGAGTACAG
mZnF4 Reverse	CTGTACTCGATGAAAGCCAGTGTGGCAAAGCCCTTG
mZnF7 Forward	ATGCCAAGTGCAACGGCTACGCCAACGAAGCCTTTCAGTTCAAGCAGATGTATGG
mZnF7 Reverse	CCATACATCTGCTTGAACTGAAAGGCTTCGTTGGCGTAGCCGTTGCACTTGGCAT
mDUB Forward	TGACGGCAATGCCCTCATGCATGCC
mDUB Reverse	GGCATGCATGAGGGCATTGCCGTCA
MYC Start Codon Removal Forward	TCAACCGGTAAGGCTAGTCTT
MYC Start Codon Removal Reverse	AAGACTAGCCTTACCGGTTGA
A20 Stop Codon Insert Forward	ATGTATGGCTGAGAACGCGTG
A20 Stop Codon Insert Reverse	CACGCGTTCTCAGCCATACAT
A20 delta OTU Forward	5’Phos-GGGCACGCCCAGAATCC
A20 delta OTU Reverse	GAATTCACTAGTAGTATGCAAATCTTCTTCAGATATCAGC
A20 delta ZnF4 Forward	5’Phos-TTTGCTGCTGCCTCAGG
A20 delta ZnF4 Reverse	CCCAGGAGTCCGTGC
A20 delta ZnF7 Forward	5’Phos-GGAGAACGCGTGGACTACAAAGACC
A20 delta ZnF7 Reverse	GGGGGCAGGCTCACCC

Primer Name	Primer Sequence (5’-3’)
A20 N-term Fragment Forward	5’Phos-TAGGCGGCCGCCTGGCC
A20 N-term Fragment Reverse	CCGAGAGGCCCCGAGCG
A20 C-term Fragment Forward	5’Phos-GGAGAAGCCTATGAGCCC
A20 C-term Fragment Reverse	CATACCGGTTGATCTCAGGTA
GFP2 Forward	TGGCAATCCGGTACTGTTGGTAAAGCCACCATGCCCGCCATGAAGATC
GFP2 Reverse	CTCCTCCACCTCGGGAGGGAAGCCGTGAGATAATCGAGCTCGAGATCTGG
NF-κB Backbone Forward	TCTCACGGCTTCCCTCCCGAGG
NF-κB Backbone Reverse	GGTGGCTTTACCAACAGTACCG
RE Excision Forward	AGATCTGGCCTCGGCGGCCAAGCTT
RE Excision Reverse	GAGCTCAGGTACCGGCCAGTTAGGCC
AP-1 RE Forward	GGCCTAACTGGCCGGTACCTGAGCTCTGAGTCAGTGACTCAGTGAGTCAGTGACTCAGTGAGTCAGTGACTCAG
AP-1 RE Reverse	GTGTCTAAGCTTGGCCGCCGAGGCCAGATCTTGATATCCTCGAGCTGAGTCACTGACTCACTGAGTCACTGAC